Mapping and Fitting the Peripheral Benzodiazepine Receptor Binding Site by Carboxamide Derivatives. Comparison of Different Approaches to Quantitative Ligand−Receptor Interaction Modeling

Maurizio Anzini,*,§ Andrea Cappelli,*,‡ Salvatore Vomero,‡ Michele Seeber,$ Maria Cristina Menziani,$ Thierry Langer,† Bertram Hagen,† Cristina Manzoni,# and Jean-Jacques Bourguignon^

Dipartimento di Scienze Farmacobiologiche, Università degli Studi "Magna Graecia" di Catanzaro, Complesso "Ninì Barbieri", 88021 Roccelletta di Borgia, Catanzaro, Italy, Dipartimento Farmaco Chimico Tecnologico, Università di Siena, Via A. Moro, 53100 Siena, Italy, Dipartimento di Chimica, Università degli Studi di Modena, Via Campi 183, 41100 Modena, Italy, Institute of Pharmaceutical Chemistry, University of Innsbruck, Innrain 52A, A-6020, Innsbruck, Austria, Istituto di Ricerche Farmacologiche "Mario Negri", Via Eritrea, 62, 20157 Milano, Italy, and Laboratoire de Pharmacochimie de la Communication Cellulaire (UMR 7081), Université Louis Pasteur, 74 Route du Rhin, 67401 Illkirch Cedex, France

Received April 28, 2000

The synthetic-computational approach to the study of the binding site of peripheral benzodiazepine receptor (PBR) ligands related to 1-(2-chlorophenyl)-*N*-methyl-*N*-(1-methylpropyl)-3-isoquinolinecarboxamide (PK11195, **1**) within their receptor (Cappelli et al. *J. Med. Chem.* **1997**, *40*, 2910−2921) has been extended. A series of carboxamide derivatives endowed with differently substituted planar aromatic or heteroaromatic systems was designed with the aim of getting further information on the topological requisites of the carbonyl and aromatic moieties for interaction with the PBR binding site. The synthesis of most of these compounds involves Weinreb amidation of the appropriate lactone as the key step. The most potent compound, among the newly synthesized ones, shows a nanomolar PBR affinity similar to that shown by **1** and the presence of a basic *N*-ethyl-*N*-benzylaminomethyl group in 3-position of the quinoline nucleus. Thus, it may be considered the first example of a new class of water soluble derivatives of **1**. Several computational methods were used to furnish descriptors of the isolated ligands (indirect approaches) able to rationalize the variation in the binding affinity of the enlarged series of compounds. Sound QSAR models are obtained by size and shape descriptors (volume approach) which codify for the short-range contributions to ligand−receptor interactions. Molecular descriptors which explicitly account for the electrostatic contribution to the interaction (CoMFA, CoMSIA, and surface approaches) perform well, but they do not improve the quantitative models. Moreover, useful hints for the identification of the antagonist binding site in the three-dimensional modeling of the receptor (direct approach) were provided by the receptor hypothesis derived by the pharmacophoric approach. The ligand−receptor complexes obtained provided a detailed description of the modalities of the interaction and interesting suggestions for further experiments.

Introduction

After the discovery of benzodiazepine binding sites in the periphery (peripheral benzodiazepine receptor, PBR), intensive research devoted to the characterization of this receptor has been undertaken.[1] PBR has been primarily found on the mitochondrial outer membrane even if a nonmitochondrial localization in some cells has been suggested. Although the physiological role of PBR is still unclear, a wide range of pharmacological activities, such as anticonvulsant, anxiolytic, immunomodulating, and cardiovascular, has been related to its activation.[2] In particular, this receptor appears to be involved in steroidogenesis, the regulation of which represents a potential clinical application of PBR ligands.[3]

Human, bovine, rat, and murine PBR have been isolated, cloned, and sequenced.[4] However, the crystallographic structure is not yet available, since its close association to the membrane makes this protein difficult to isolate, purify, and crystallize in its native form.

Models of the secondary[5] and tertiary[6] structure of the PBR available in the literature are essentially concerned with the transmembrane region (TM), which consists of five α-helices composed of 21 hydrophobic residues. The N-terminus of the sequence is located in the mitochondrial domain, while the C-terminus is exposed to the cytoplasm. The transmembrane regions are connected by loops rich in hydrophilic residues. Furthermore, recently reported site-directed mutagenesis studies demonstrated that the portion of the receptor involved in the interaction with the ligands mainly consists of the first cytoplasmic loop and that agonists and antagonists bind the receptor in different, albeit partly overlapping, sites.[7]

* To whom correspondence should be addressed. Anzini, M. Tel: +39 961 391157. Fax: +39 961 391490. E-mail: anzini@unicz.it. Cappelli, A. Tel: +39 577 234320. Fax: +39 577 234333. E-mail: cappelli@unisi.it.
§ Dipartimento di Scienze Farmacobiologiche, Università "Magna Graecia" di Catanzaro.
‡ Dipartimento Farmaco Chimico Tecnologico, Università di Siena.
$ Dipartimento di Chimica, Università degli Studi di Modena.
† Institute of Pharmaceutical Chemistry, University of Innsbruck.
# Istituto di Ricerche Farmacologiche "Mario Negri".
^ Laboratoire de Pharmacochimie de la Communication Celluleire, Université Louis Pasteur.

10.1021/jm0009742 CCC: $20.00
Published on Web 03/20/2001

Chart 1

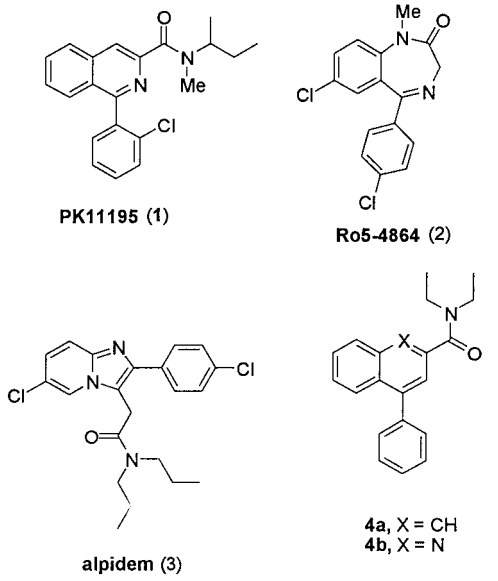

PK11195 (**1**, Chart 1) is the first nonbenzodiazepine ligand which was found to bind the peripheral benzodiazepine receptors (PBR) with nanomolar affinity, and it is nowadays the most commonly used radioligand for this receptor along with Ro5-4864 (**2**). The class of high affinity PBR ligands also comprises alpidem (**3**), an imidazopyridine, capable of stimulating pregnenolone formation from mitochondria of C6-2B glioma cells.[3] The structure−affinity relationship data of the analogues of **1** (e.g., compounds **4a**,**b**) were reported in the patent by Dubroeucq and co-workers and were later discussed by Bourguignon.[8] Georges and co-workers studied a limited set of **1**-like compounds by means of molecular orbital calculations in the attempt to define and map the PBR binding site.[9]

Our earlier efforts in the search of new PBR ligands culminated in the discovery of some new lead compounds **5** and **6**, providing submicromolar affinity and possessing some structural similarity with **1**.[10] With the aim of both understanding the interaction of leads **5** and **6** with the PBR binding site at molecular level and optimizing their PBR affinity, we planned a large program focused on the structural modification of these compounds.

In a previous paper,[11] we presented the results of a synthetic-computational approach which, by means of the conformationally constrained derivatives **7**−**11** (Chart 2), afforded important information on the orientation of the carbonyl group of compound **1** in the interaction with the PBR binding site.

Furthermore, compounds **8f**−**h** (see Table 1) have been [^{11}C]-labeled as PET PBR ligands potentially useful in the imaging of multiple sclerosis, human glyoma and glyoblastoma, cerebral infarction, and calcium channel anomalies in heart diseases.[12]

The present paper deals with the complementary information obtained by structural modification of the carboxylic ester moiety, the *N*-ethyl-benzylamino group, and the heteroaromatic system of compounds **6**. Several computational methodologies have been applied to the enlarged series of published (**7**−**11**) and newly designed (**12**−**16**, Chart 3) compounds in order to rationalize the

Chart 2

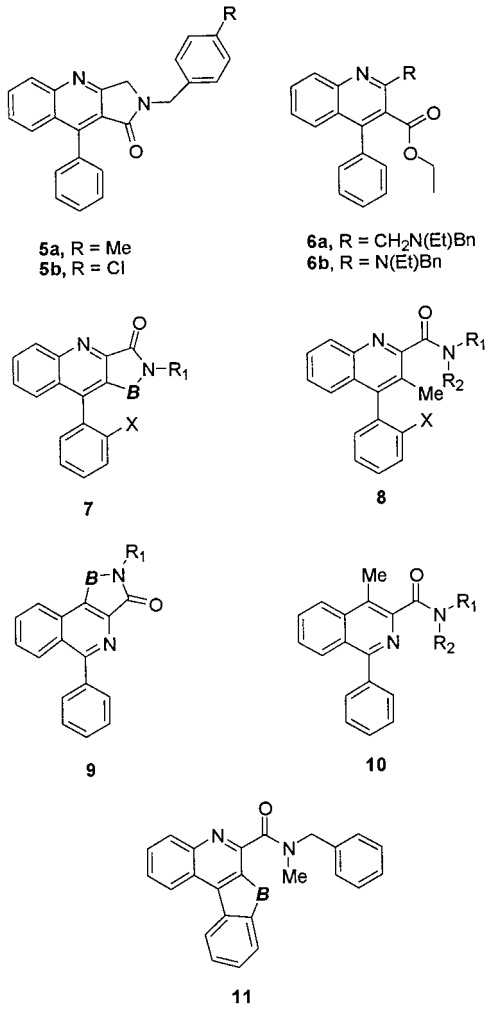

variation in their binding affinities. First, the indirect approach has been carried out on the isolated ligands. The molecular determinants for the interaction with the receptor have been inferred from the comparison of the van der Waals volume (volume approach), the steric and electrostatic fields (CoMFA and CoMSIA approaches), and the molecular surface electrostatic potentials (surface approach) of each ligand with respect to one or more reference compounds. Moreover, the adequacy of each ligand to a specific pharmacophoric hypothesis (pharmacophoric approach) has also been exploited to obtain molecular descriptors for quantitative structure−activity relationship (QSAR) analysis. The (QSAR) models developed have been tested for their predictive power by means of compound **16**, which can be considered a structural hybrid between the first and the second set of the PBR ligands studied.

Finally, the clues obtained by the indirect approach have been exploited, together with the experimental information available on the receptor, to obtain three-dimensional models of the ligand−receptor complexes (direct approach) which provide a detailed description of the interaction modalities and interesting suggestions for further experimental investigation.

Chemistry

Carboxamides **13a**−**g**, **15a**−**d,** and **16** were obtained by the multistep sequence shown in Scheme 1. The

Table 1. PBR Binding Affinities of Previously Described Compounds **7**−**11**

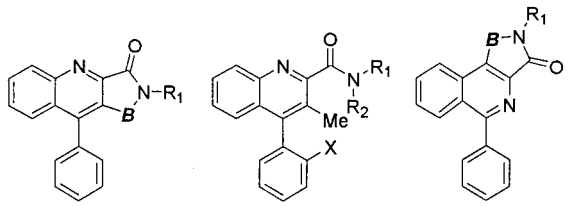

7 **8** **9**

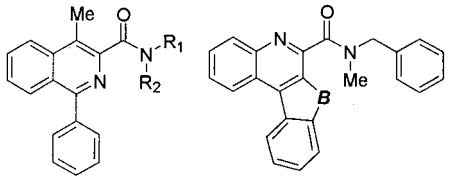

10 **11**

compd	bridge (***B***)	X	R_1	R_2	IC_{50} (nM) ± SEM[a]
7a	*n*-Bu-CH		Bn		810 ± 110
7b	CH_2-CH_2-CH_2		*s*-Bu		1200 ± 200
7c	CH_2-CH_2-CH_2		Bn		170 ± 14
8a		H	*s*-Bu	H	230 ± 70
8b		F	*s*-Bu	H	13 ± 4.9
8c		H	Bn	H	1200 ± 180
8d		H	4-Cl-Bn	H	1700 ± 230
8e		F	4-Cl-Bn	H	270 ± 66
8f		H	*s*-Bu	Me	2.1 ± 0.9
8g		F	*s*-Bu	Me	2.9 ± 0.5
8h		H	Bn	Me	2.1 ± 0.6
8i		H	4-Cl-Bn	Me	9.8 ± 2.0
8j		F	4-Cl-Bn	Me	3.4 ± 1.0
8k		H	4-Cl-Ph	Me	6.4 ± 1.1
8l		H	4-MeO-Ph	Me	8.8 ± 1.5
9a	CH_2		*s*-Bu		620 ± 100
9b	CH_2		Bn		480 ± 29
9c	CH_2-CH_2-CH_2		*s*-Bu		780 ± 20
9d	CH=CH-CH_2[b]		*s*-Bu		490 ± 47
9e	CH=CH-CH_2[b]		Bn		45 ± 15
10a			*s*-Bu	H	550 ± 93
10b			*s*-Bu	Me	11 ± 2.6
10c			Bn	Me	3.1 ± 0.8
11a	CH_2-CH_2				8.9 ± 2.5
11b	O-CH_2-CH_2[b]				10 ± 0.7
1					2.2 ± 0.3

[a] Each value is the mean ± SEM of three determinations. [b] See ref 11.

appropriate lactone (9-phenylfuro[3,4-*b*]quinoline-1(3*H*)-one (**17**),[13] 9-phenylfuro[3,4-*b*]quinoline-3(1*H*)-one (**18**),[13] and commercially available phthalide **19**) underwent aminolysis with the suitable aluminum amide reagent (AAR) as the key step[14] to afford the corresponding hydroxymethylcarboxamides **20a**−**e**, **21**, and **22a**−**d** (method A). On the other hand, 2-hydroxymethyl-3-quinolinecarboxamides **20f** and **20g** were obtained by ring opening of lactone **17** with the highly reactive propylamine and benzylamine, respectively (method B).

By treatment of the hydroxymethylcarboxamides **20a**−**g**, **21**, and **22a**−**d** with thionyl chloride in methylene chloride, chloromethyl derivatives **23a**−**g**, **24**, and **25a**−**d** were obtained and easily converted into corresponding final products **13a**−**g**, **15a**−**d**, and **16** by means of *N*-ethylbenzylamine.

Compound **12b** was prepared by alkylation of 1,2,3,4-tetrahydroisoquinoline with the previously reported 3-carbethoxy-2-chloromethyl-4-phenylquinoline[13] according to the standard methods, while carboxamides

Chart 3

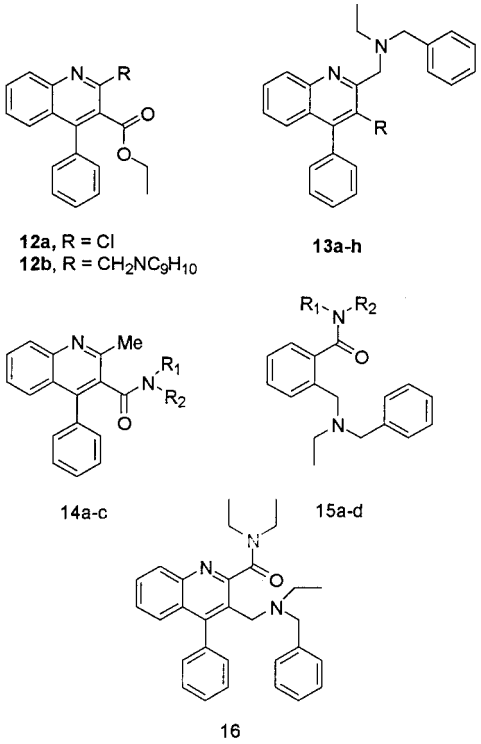

12a, R = Cl
12b, R = $CH_2NC_9H_{10}$

13a-h

14a-c **15a-d**

16

Scheme 1[a]

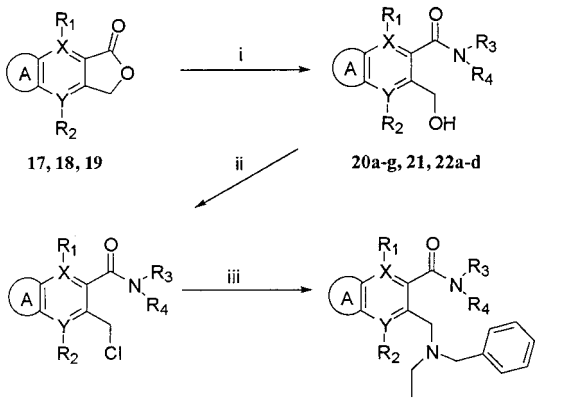

17, 18, 19 **20a-g, 21, 22a-d**

23a-g, 24, 25a-d **13a-g, 15a-d, 16**

compd	A	X	Y	R_1	R_2	R_3	R_4
17	C_6H_4	C	N	Ph			
18	C_6H_4	N	C		Ph		
19		C	C				
13a, 20a, 23a	C_6H_4	C	N	Ph		Me	Me
13b, 20b, 23b	C_6H_4	C	N	Ph		Et	Et
13c, 20c, 23c	C_6H_4	C	N	Ph		*n*-Pr	*n*-Pr
13d, 20d, 23d	C_6H_4	C	N	Ph		Me	Ph
13e, 20e, 23e	C_6H_4	C	N	Ph		Me	4-Cl-Ph
13f, 20f, 23f	C_6H_4	C	N	Ph		H	*n*-Pr
13g, 20g, 23g	C_6H_4	C	N	Ph		H	Bn
15a, 22a, 25a		C	C			Me	Me
15b, 22b, 25b		C	C			Et	Et
15c, 22c, 25c		C	C			*n*-Pr	*n*-Pr
15d, 22d, 25d		C	C			Me	Ph
16, 21, 24	C_6H_4	N	C		Ph	Et	Et

[a] Reagents: (i) Method A: Me_3Al, $R_3(R_4)NH{\cdot}HCl$, CH_2Cl_2, Method B: R_4NH_2, EtOH; (ii) $SOCl_2$, CH_2Cl_2; (iii) Bn(Et)NH, NaI, Na_2CO_3, MeCN.

14a−**c** were synthesized as reported in Scheme 2. Ester **26**[15] was hydrolyzed in basic medium to yield corresponding acid **27**[16] which was first reacted with phosphorus pentachloride in methylene chloride and then

Scheme 2[a]

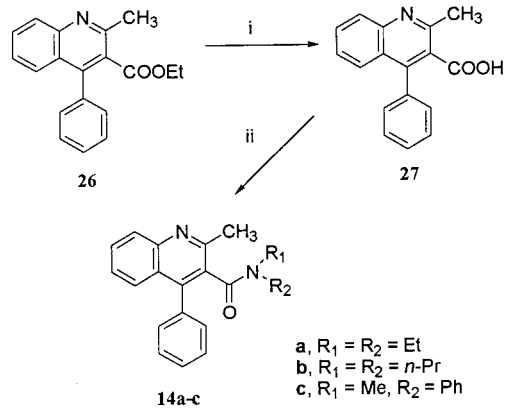

[a] Reagents: (i) 3 M NaOH, $CH_3OCH_2CH_2OH$; (ii) (a) PCl_5, CH_2Cl_2, (b) $R_1(R_2)NH$, CH_2Cl_2, Na_2CO_3 (10% sol).

with the suitable secondary amine in the presence of Na_2CO_3 to afford the expected carboxamide.

Bromination of 2-methyl-4-phenylquinoline[16a] with NBS in the presence of dibenzoyl peroxide gave 2-bromomethyl-4-phenylquinoline (**28**) which was converted into the tertiary amine **13h** by reaction with *N*-ethylbenzylamine in ethanol at reflux in the presence of K_2CO_3.

Computational Procedures

The structures of the studied compounds were optimized using the semiempirical AM1 method[17] within the MOPAC 6.0 (QCPE 455) program. The molecular mechanics correction to amide bond was applied. The three-dimensional structure of compound **9d**, solved by X-ray crystallography, was used as an input for the geometry optimization.[11] The molecules containing atoms inclined to be protonated were considered in both their charged and neutral forms. Enantiomer *R* was arbitrarily chosen for compounds showing an asymmetric carbon in their structures since both *R* and *S* enantiomers of PK11195 (**1**) were found to be nearly equipotent toward PBR [(*R*), IC_{50} = 9 nM; (*S*), IC_{50} = 19 nM; (*R*,*S*), IC_{50} = 9 nM)].[8]

Molecular Alignment Used in Volume, Surface, and Pharmacophore Approaches. Since two noncongeneric molecular sets were considered, we evaluated two different methods for ligand alignment in the indirect approaches.

In the first we proceeded to a topological alignment on the basis of the ligand common quinoline or isoquinoline nucleus. Whenever that fragment was absent, the benzene ring directly bound to the carbonyl group was used.

In the second, we used dummy atoms appropriately located so that the hypothetical interactions with residues on the receptor counterpart could be considered: a dummy atom on the vector defined by the carbonyl group, 1 Å away from the oxygen; two dummy atoms 2 Å above and below the center of the common bond of the bicyclic aromatic group, perpendicularly oriented with respect to the plane defined by the aromatic moiety; two dummy atoms 2 Å above and below the center of the pendant phenyl group. The alignment was carried out by rms minimization of the distance between the dummy atoms of the different molecules with respect to those of the target ligands. As for the molecules of the second set which did not have the reference fragments, we proceeded to the topological alignment with the closest compound that allowed the definition of all dummy atoms.

Volume Approach. Compounds **8f**, **8h**, and **10c** were taken as templates when building the reference supermolecule. These are the most structurally different ligands which show high affinity for the PBR. The van der Waals volume of the supermolecule was then computed with the molecular modeling program Quanta.[18] All the other compounds satisfactorily matched their analogous ligands constituting the supermolecule by using their global minimum conformer or conformers, the energy of which is only 1 kcal/mol above the global minimum. The best QSAR equations are obtained by the topological alignment. The following ad-hoc defined size and shape descriptors were calculated:

V_{in} = van der Waals volume of the ligands included in the supermolecule van der Waals volume.

V_{out} = excluded van der Waals volume with respect to the supermolecule volume.

$V_{dif} = (V_{in} - V_{out})/V_{sup}$, the difference between the above two values normalized to the total supermolecule volume.

Surface Approach. A surface enclosing the aggregate aligned ligands, **8f**, **8h**, and **10c** was generated by means of the program Receptor.[18]

To this purpose, a Wyvill soft object function was used.[19] Regions of the receptor surface model were removed at zones which proved to accept substitution. Molecular alignment was achieved both by topologically superimposing the ligands and by using the previously defined dummy atoms. In the Results and Discussion section we reported the results obtained with the second method, since the receptor surface obtained in this way better rationalizes the observed binding affinity variation in this molecular series of compounds.

The receptor surface model supports energetic calculations for the interactions of molecules with the model. The evaluation was performed on the basis of the electrostatic potential. The neutral form was considered for the compounds containing basic atoms. The solvation correction, which adds a penalty function whenever polar atoms are placed in hydrophobic regions of the receptor surface model, did not appear to improve the results.

Each ligand was subjected to a few minimization steps within the model to avoid excessive penalization of those molecules whose minimum conformation is not compatible with the receptor cavity obtained. It is noteworthy that the conformation taken up by the ligands inside the receptor may actually be quite different from the minimum conformation of the isolated molecule; therefore, conformers characterized by an energy of 2 kcal/mol above the isolated molecule energy minimum were accepted.

The total interaction energy (E_{inter}) of the molecule with the receptor surface model turned out to be the most interesting descriptor among those calculated by the program.

Pharmacophore Approach. Compounds **8f**, **8h**, and **11a** were chosen to generate a pharmacophoric hypothesis with the Catalyst program.[18] Compound **11a**

was chosen because of the peculiar position of its pendant phenyl group. Four pharmacophoric groups were used in the model generation process. They are as follows: (a) one hydrogen bond donor (carbonyl group); (b) one aromatic ring corresponding to the pendant phenyl group; (c) one aromatic ring corresponding to the phenyl ring of the quinoline nucleus farthest from the above-mentioned pendant phenyl ring; (d) one hydrophobic group corresponding to the aromatic or aliphatic chains bound to the amide group.

The mutual positions of the pharmacophoric features were mapped in the 3D space, and a weight was assigned to each atom on the basis of structure−affinity relationship (SAFIR) considerations. Thus, we lowered the tolerance of the hydrogen bond acceptor, since the carbonyl position is very important for the recognition of the ligands,[11] and we allowed more freedom to the aromatic ring defining the pendant phenyl. Of the various models (hypotheses) obtained, the ones showing the highest space occupancy of the pharmacophoric groups were chosen. The AM1 minimized structures of the ligands were then evaluated on the basis of the hypothesis selected.

In the evaluation process, the program considers how each molecule fits the number and space disposition of the pharmacophores present in the receptor hypothesis and gives a score called *Fit* of the molecule.

PBR Receptor Modeling. Human, bovine, murine, and rat PBR sequences were retrieved from the protein sequences EMBL database (http://www.embl-heidelberg.de/srs5). The human PBR hydropatic profile analysis was performed by means of the TopPred method (http://www.biokemi.su.se/~server/toppred2/toppredserver.cgi). The search for three-dimensionally resolved analogous proteins was performed by means of the SCOP program (http://scop.rmc-lmb.cam.ac.uk/scop).

The modeling of the receptor and of the complexes was performed with the QUANTA program.[18] The complete PBR model was obtained by considering the structural restraints drawn by the Apolipophorin III (pdb code: 1aep) for the transmembrane region and by the V9-K27 portion of the Myohemerythrin (pdb code: 2mhr) for the first loop, while the third loop of the C-terminal part of the receptor was modeled "ab initio" by considering the conformational preferences of the short stretch of the amino acids. The Modeller program[20] deduces distance and angle constraints from the target sequences and combines them with energy terms for an adequate stereochemistry in an objective function, later optimized in the Cartesian space by conjugate gradients and molecular dynamics (simulated annealing) methods. Different models of the PBR receptor were generated through randomization of the Cartesian coordinates of all the atoms, with a deviation of ±4 Å. Minimization of the structures was achieved by means of CHARMm program.[21] The minimization procedure consisted of 200 steps of steepest descent followed by a conjugate gradient minimization up to a potential energy value of <0.0001 kcal/mol Å. We used the united atom force field parameters and a dielectric constant value of 80, since we were interested in the loop portions of the receptor. The interaction energies at the binding site were calculated with a dielectric constant $\epsilon = 4r$. A technical check of the quality of the model was performed by means of the Protein Health utility (Ramachandran plots for main chain and side chain conformations, chirality, solvent accessibility of polar, hydrophilic and hydrophobic atoms, close contacts, and holes) and the 3D Profile Analysis program [22] within the Quanta[18] framework.

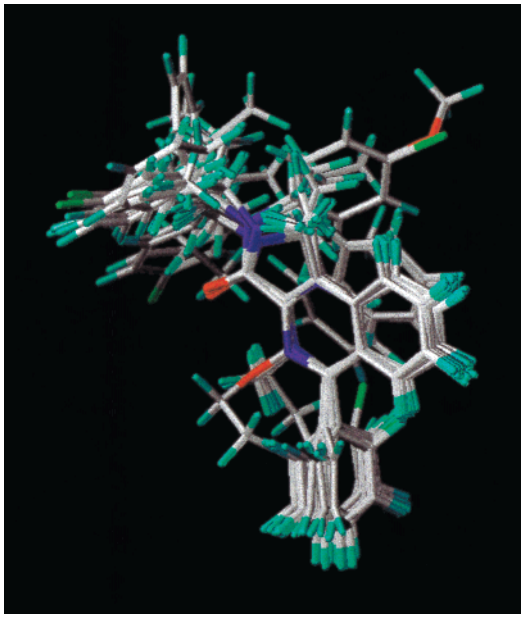

Figure 1. Structural alignment of compounds **8**−**11** for the calculation of CoMFA and CoMSIA.

CoMFA. A CoMFA[23] model was developed using previously described compounds **8**−**11**.[24] The molecular structures of the ligands under investigation were refined by using the Tripos force field parameter set available within version 6.3 of the SYBYL molecular modeling software package.[25] Conformational analysis was performed using molecular dynamics together with simulated annealing, and the geometry of all structures retrieved at low temperature was fully optimized using the conjugate gradient algorithm with a convergence criterion of 0.0001 kcal/mol Å. The most rigid compounds in this series proved to be **9d**,**e**. Both structures possess a double bond that reduces flexibility in the fused azepine ring of the isoquinoline system. Compound **9e** is the slightly more active compound, with an IC_{50} value of 45 nM. The minimum energy conformer was selected as a reference structure. In this conformer a torsion angle of −149° was found between the carboxyl-oxygen atom of the azepine ring and the planar aromatic isoquinoline ring system. This torsion angle (±10°) could also be found at all the other compounds of the set. The alignment for CoMFA was done by manually fitting the atoms of the aromatic heterocycle of minimum energy structures with their amide function exhibiting an appropriate torsion angle to the planar part of the molecule (Figure 1). For the interaction energy matrix calculation, the default CoMFA atom probe parameters were used (i.e., the Lennard-Jones potential of a sp^3 type carbon atom [C.3] and charge +1) and the values were scaled accordingly by means of the standard CoMFA scaling. The regression analysis was performed by means of partial least-squares (PLS) method.[26] To establish the quality of the CoMFA derived, cross-validation was done by means of the leave-one-out method. An r^2_{cv} of 0.592 was found

(s_{PRESS}: 0.720 (three components), $n = 23$), indicating an acceptable predicting capability of the model. The final model without validation was found to give a conventional r^2 of 0.949 ($s = 0.254$, $n = 23$) and was used for affinity prediction of newly synthesized compounds **13b** and **16**. The affinity values of compounds **13b** and **16** (containing an amino function) were predicted with the molecules both in the neutral and in the protonated form.

CoMSIA. Another 3D QSAR model was developed based on previously described compounds **8**−**11** by means of the CoMSIA approach.[27] The same structural alignment as for the CoMFA was taken, and the default attenuation factor (0.3) was selected for the similarity index calculation in steric and electrostatic fields. The regression analysis was performed by means of PLS. To determine the quality of the CoMSIA derived, cross-validation was done by means of the leave-one-out method. An r^2_{cv} of 0.538 was found (s_{PRESS}: 0.784 (three components), $n = 23$), indicating a predicting capability comparable to the CoMFA method. The final model without validation was found to give a conventional r^2 of 0.908 ($s = 0.334$, $n = 23$) and was used for affinity prediction of the newly synthesized compounds **13b** and **16**. The affinity values of compounds **13b** and **16** (containing an amino function) were predicted with the molecules both in the neutral and in the protonated form.

Results and Discussion

Structure−Affinity Relationships. The importance of the carbonyl group in the interaction of PBR ligands with their receptors has been stressed by several authors.[3,8,9] This is one of the most important groups in the structure of **1** which is, in principle, capable of giving long-range (strong and directional) electrostatic interactions with the receptor.

In a previous paper we described the results obtained in a series of conformationally constrained carboxamide derivatives **7**−**11** (see Table 1).[11] These compounds are closely related to **1**, while they differ from compounds **6** because the amide moiety is attached to C-2 of the bicyclic heteroaromatic system instead of C-3 as in compounds **6**. The work performed on conformationally constrained derivatives **7**−**11** confirmed the essential role of the carbonyl function as the primary pharmacophoric element, and the importance of the role of both the amide substituents and the pendant phenyl ring for which a dispersive nature of the interactions with PBR binding site was suggested.

To obtain information on the binding modalities of compounds **6**, their main structural features (the carboxylic ester moiety, the *N*-ethylbenzylamino group, and the bicyclic heteroaromatic system with the pendant phenyl ring) were subjected to structural modification.

The newly synthesized compounds (**12**−**16**) were tested for their potential ability to displace [^{3}H]-**1** from PBR in rat brain cortex (in the same test system used for compounds **7**−**11**) in comparison with **1**, and the results of these studies are summarized in Table 2.

The results obtained clearly show that the replacement of the ester function of **6a** with a secondary (**13f**) or tertiary amides (**13a**−**c**) affords compounds with similar micromolar range affinities, when compared with ester **6a**. In addition, the environment of the carbonyl amide seems to be relatively sensitive to steric hindrance since the increase in size of the amide substituents results in a progressive decrease in affinity (compare compounds **13b**−**e** with **13a**). These findings appear to be in disagreement with the results described in the literature.[3,8] Moreover, although the variation in the PBR affinity consequent to the removal of the lipophilic amide group in compounds **13a**,**b** (compare **13a**,**b** with **13h**) is significant and suggests a specific role of this group in the ligand−receptor interaction, our work (see also ref 11) clearly shows that a suitably oriented lipophilic amide group plays a more substantial role and contributes to the binding strength much more than the one in the 3-position of the quinoline nucleus of **13a**−**g**. Taken together, these results suggest that the lipophilic amide groups in 3-position of the quinoline nucleus of compounds **13a**−**g** occupy a receptor area

Table 2. PBR Binding Affinities of Compounds **4**−**6** and **12**−**16** [IC_{50} (nM) + SEM][a]

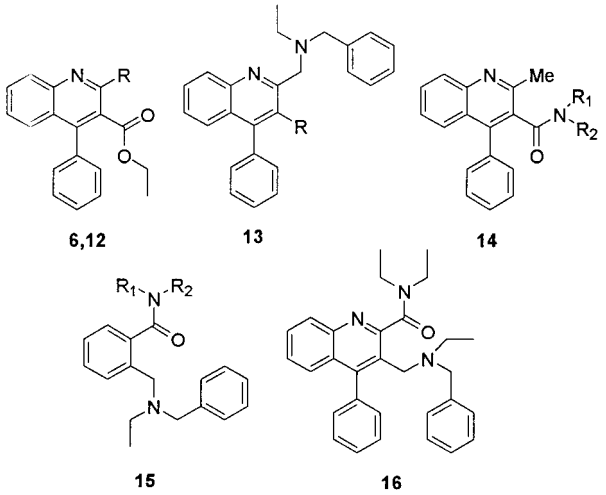

compd	R	R_1	R_2	IC_{50}
4a[b]				5
4b[b]				27
5a[b]				410
5b[b]				210
6a[b]	$CH_2N(Et)Bn$			700
6b[b]	N(Et)Bn			540
12a[c]	Cl			3700 ± 250
12b	CH_2THIQ[d]			1185 ± 134
13a	$CONMe_2$			229 ± 44
13b	$CONEt_2$			373 ± 58
13c	CON(*n*-Pr)$_2$			456 ± 132
13d	CON(Me)Ph			1317 ± 367
13e	CON(Me)4-Cl-Ph			2479 ± 360
13f	CON(H)*n*-Pr			872 ± 293
13g	CON(H)Bn			2895 ± 532
13h	H			3400 ± 280
14a		Et	Et	>10000
14b		*n*-Pr	*n*-Pr	>10000
14c		Me	Ph	>10000
15a		Me	Me	>10000
15b		Et	Et	8209 ± 1016
15c		*n*-Pr	*n*-Pr	8867 ± 1164
15d		Me	Ph	>10000
16				4.1 ± 1.03
1				2.2 ± 0.3

[a] Each value is the mean ± SEM of three determinations. [b] The IC_{50} value of these compounds was taken from the literature (**4a**,**b**: see ref 8; **5a**,**b** and **6a**,**b**: see ref 10). [c] See ref 10. [d] THIQ = (1,2,3,4-tetrahydroisoquinolin)-2-yl.

different from the one occupied by the lipophilic amide groups of the high affinity PBR ligands.

Comparison of compounds **6a**,**b** with **12a** and **13h** suggested that the *N*-ethylbenzylamino group of **6a,b** plays a significant role in the interaction of these compounds with PBR. To characterize better the role of the benzylamino side chain in these compounds, a short series of 2-methyl derivatives was prepared (**14a**−**c**). Their inactivity highlights the importance of the presence of a large lipophilic substituent in the 2-position of the bicyclic heteroaromatic system (compare **14a**−**c** with **13b**−**d**) for the binding to PBR. It is also noteworthy that inclusion of the *N*-ethylbenzylamino group into a rigid tetrahydroisoquinoline ring did not significantly modify the affinity (compare compound **6a** with **12b**).

The bicyclic heteroaromatic system with the pendant phenyl ring of phenylquinolinecarboxamides **13a**−**g** also plays a major role in the molecular recognition process as its simplification into a benzo ring led to the significantly less potent ligands **15** (compare **13b**−**d** with **15a**−**c**).

The integration of the information obtained from the SAFIR analysis discussed above with that obtained from conformationally constrained derivatives **7**−**11** led to the design of the positional isomer of **13b** in which the substituents in positions 2 and 3 of the quinoline nucleus are inverted (compound **16**). It is interesting to note that carboxamide derivative **16**, bearing a *N*-ethylbenzylamino group in the 3-position of the quinoline nucleus, shows a nanomolar PBR affinity comparable with that shown by **1**.

On the whole, these findings lead to some considerations: (a) the presence of a carbonyl dipole suitably located (e.g., in 2-position of the bicyclic aromatic system) and oriented (e.g., in perpendicular position with respect to the bicyclic system) is needed for high PBR affinity; (b) lipophilic substituents attached (directly or rather by interposition of -C(═O)-N- fragment) to the 2-position are favorable for the interaction with PBR; (c) the presence of a bicyclic aromatic or heteroaromatic system bearing a suitably located pendant phenyl ring is of fundamental importance for the interaction with PBR; (d) a zone of tolerance to large substituents seems to be located in the PBR site interacting with the 3-position of quinoline nucleus; and (e) the PBR binding site seems to tolerate well the positive charge presumably borne by the tertiary amine nitrogen of **16** at physiological pH. These considerations on the PBR interaction of carboxamide derivatives related to **1** are easily translated into the interaction model of compound **16** shown in Figure 2.

Quantitative Structure−Affinity Relationships (QSAR). (a) Receptor Mapping. To obtain a quantitative rationalization of the structure−affinity relationships, it is of primary importance to define molecular descriptors with high information content. A good quantitative rationalization of the affinity variation of 26 molecules in the series of compounds **7**−**11** has recently been obtained[11] through comparison of the van der Waals volumes of the different ligands with that of an ad-hoc defined reference supermolecule.[28]

In this approach we assume that the volume obtained by superimposing the most structurally different ligands showing the highest affinities reflects the overall shape and conformational freedom of the PBR binding site. Thus, compounds **8f**, **8h**, and **10c** were chosen to constitute the supermolecule and were topologically superimposed as described in the methods section.

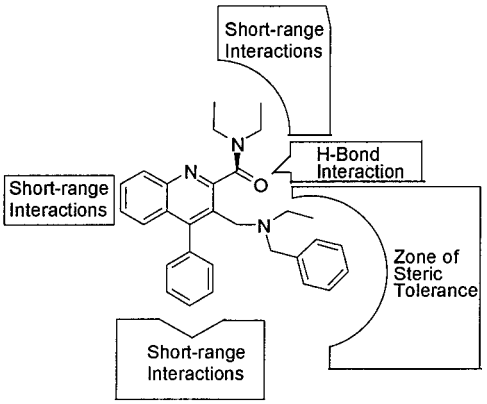

Figure 2. Schematic representation of the interactions of compound **16** with the PBR binding site.

Molecular descriptors such as V_{in}, V_{out}, and V_{dif} were then calculated. V_{in} and V_{out} are, respectively, the inner and outer van der Waals molecular volumes of the ligands considered with respect to the resultant reference volume of the supermolecule, and, from an interpretative point of view, they mimic the short-range attractive (V_{in}) and repulsive interactions (V_{out}) with the receptor. V_{dif} is defined as the difference between V_{in} and V_{out} and is normalized with respect to the volume of the supermolecule.

The V_{dif} descriptor gave the most significant results, as shown by the previously reported[11] QSAR model developed for compounds **7**−**11**

$$pIC_{50} = 10.25(\pm 0.97)V_{dif} + 1.43(\pm 0.56) \qquad (1)$$

$$n = 26, \quad r^2 = 0.83, \quad s^2 = 0.21, \quad F = 111.09$$

where n is the number of compounds considered, r the correlation coefficient, s the standard deviation, and F the value of the Fisher ratio; the numbers in parentheses are 95% confidence intervals of the regression coefficient and of the intercept.

Recalling the mathematical formulation of this molecular descriptor, the correlation suggests that, in the molecular series of the compounds considered, the binding affinities are modulated by the molecular shape of the amide substituents through the optimization of dispersive and steric interactions.

The previously chosen supermolecule is surprisingly able to rationalize the affinity of the additional ligands considered in this work. The following correlation is obtained by considering the ligands of Table 3:

$$pIC_{50} = 5.86(\pm 0.58)V_{dif} + 4.09(\pm 0.28) \qquad (2)$$

$$n = 44, \quad r^2 = 0.71, \quad s^2 = 0.36, \quad F = 103.28;$$

16 omitted

However, the model fails to predict the behavior of compound **16** (Figure 3). This ligand is the only one in the quinoline set with a basic nitrogen having a high affinity for the peripheral benzodiazepine receptor. The

Table 3. PBR Affinity Indexes (pIC_{50}) and Molecular Descriptors for Compounds **1**, **4**−**13**, **15**, and **16**

compd	pIC_{50}	V_{dif}	V_{out} (Å^3)	V_{in} (Å^3)	E_{inter} (kcal/mol)	Fit
1	8.50	0.62	13.75	285.00	−3.21	3.68
4a	8.30	0.51	60.37	282.88	−3.18	3.83
4b	7.57	0.48	63.75	274.25	−3.30	3.81
5a	6.39	0.37	120.75	281.13	−1.98	2.57
5b	6.68	0.37	120.38	282.00	−1.70	2.51
6a	6.15	0.35	111.50	265.88	5.36	2.41
6b	6.27	0.29	137.62	264.63	−1.84	2.33
7a	6.09	0.43	86.38	274.00	−3.38	2.67
7b	5.92	0.54	37.50	270.38	−3.08	2.80
7c	6.77	0.52	50.75	277.63	−3.26	2.58
8a	6.64	0.49	38.12	250.88	−2.80	2.24
8b	7.89	0.62	11.63	282.50	−2.83	3.53
8c	5.92	0.46	53.00	253.25	−3.11	2.12
8d	5.77	0.43	64.25	252.75	−1.76	2.15
8e	6.57	0.50	52.00	269.38	−1.93	2.15
8f	8.68	0.70	0.00	304.00	−3.09	4.00
8g	8.54	0.69	4.88	304.75	−3.23	4.00
8h	8.68	0.74	0.00	322.63	−3.45	3.82
8i	8.01	0.66	23.75	308.88	−3.45	3.86
8j	8.47	0.67	23.75	314.88	−3.31	3.86
8k	8.19	0.59	29.50	287.75	−3.49	3.76
8l	8.06	0.57	40.63	288.00	−3.48	3.78
9a	6.21	0.44	42.87	234.88	−1.34	2.20
9b	6.32	0.45	50.13	246.50	−2.05	2.58
9c	6.10	0.53	38.62	270.88	−2.26	2.62
9d	6.31	0.53	35.25	268.25	−1.81	2.92
9e	7.34	0.55	42.75	280.50	−2.44	3.27
10a	6.26	0.51	31.50	255.63	−2.73	2.55
10b	7.95	0.65	10.13	294.50	−3.41	3.08
10c	8.51	0.74	0.00	321.50	−3.96	3.28
11a	8.05	0.60	31.62	291.88	−3.53	3.11
11b	8.00	0.63	28.88	304.50	−3.70	3.62
12a	5.43	0.38	55.87	224.38	−2.34	2.38
12b	5.92	0.48	98.12	310.63	−2.12	2.86
13a	6.64	0.35	135.25	289.50	−1.64	2.38
13b	6.43	0.31	160.25	295.13	8.14	2.77
13c	6.34	0.24	191.00	295.38	−3.06	2.66
13d	5.89	0.27	183.63	303.00	5.84	2.89
13e	5.60	0.22	201.75	299.88	10.21	2.83
13f	6.06	0.28	157.63	279.75	2.96	2.34
13g	5.54	0.21	197.50	288.88	13.58	2.67
13h	5.47	0.34	108.63	255.75	−1.32	2.25
15b	5.09	0.14	138.62	198.63	−3.57	1.98
15c	5.05	0.15	150.25	217.63	−1.11	1.93
16	8.39	0.21	205.50	296.25	−3.51	3.74

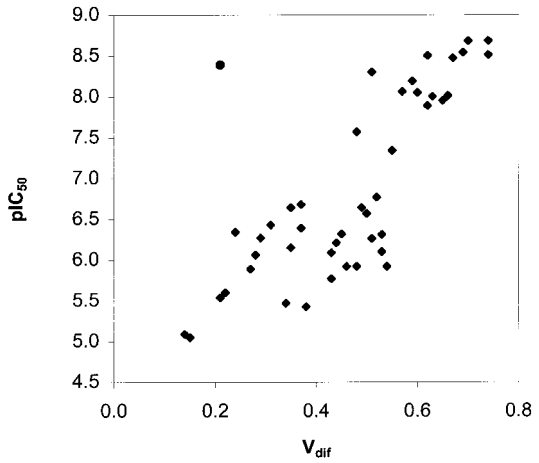

Figure 3. Correlation between the PBR binding affinity (pIC_{50}) and the V_{dif} descriptor. Compound **16,** not included in the regression, is represented as ●.

failure is probably due to the nature of the supermolecule used, which tolerates only a limited steric bulk in position 3 of the quinoline nucleus (or, more generally, additional steric bulk).

Table 4. Comparison of Experimental versus Predicted Affinities of Compounds **1**, **8**−**11** (Learning Set), **13b**, and **16** (Test Set) from CoMFA and CoMSIA Models

compd	IC_{50} (nM) ± SEM	CoMFA pred IC_{50} (nM) neutral	CoMFA pred IC_{50} (nM) NH^+	CoMSIA pred. IC_{50} (nM) neutral	CoMSIA pred. IC_{50} (nM) NH^+
1	2.2 ± 0.3	2.0		6.7	
8a	230 ± 70	94		118	
8b	13 ± 4.9	25		24	
8c	1200 ± 180	1123		770	
8d	1700 ± 230	2950		1492	
8e	270 ± 66	93		93	
8f	2.1 ± 0.9	4.1		8.4	
8g	2.9 ± 0.5	2.5		2.4	
8h	2.1 ± 0.6	2.4		5.3	
8i	9.8 ± 2.0	5.3		13	
8j	3.4 ± 1.0	4.6		2.4	
8k	6.4 ± 1.1	5.8		9.8	
8l	8.8 ± 1.5	3.8		7.3	
9a	620 ± 100	709		378	
9b	480 ± 29	887		2938	
9c	780 ± 20	516		261	
9d	490 ± 47	265		381	
9e	45 ± 15	65		43	
10a	550 ± 93	441		539	
10b	11 ± 2.6	17		8.2	
10c	3.1 ± 0.8	4.0		1.3	
11a	8.9 ± 2.5	10		13.8	
11b	10 ± 0.7	24		12.7	
13b	373 ± 58	151	132	177	2397
16	4.1 ± 1.0	44	13	13	7

On the other hand, both CoMFA and CoMSIA models developed on compounds **8**−**11** exhibit a satisfactory performance in the affinity prediction for compound **16** (Table 4). Interestingly, the affinity of compound **13b** (the positional isomer of **16**) appears to be even better predicted by the CoMFA model and by the CoMSIA model in the case of the neutral molecule. Thus, the 3D-QSAR models (CoMFA and CoMSIA) obtained appear to predict quite correctly the affinity of molecules showing significant structural differences with respect to those considered in the training set. In particular, it should be stressed that the training set is composed of molecules having lipophilic amide side chains in the 2-position of the quinoline nucleus (or equivalent) and small substituents in the 3-position, while a bulkier and basic *N*-ethylbenzylamino group is present in the 3-position of the quinoline nucleus of **16** and a lipophilic amide side chain occupies the 3-position of the quinoline nucleus of **13b**. Taken together, these observations suggest that either these 3D-QSAR models tolerate quite well the additional steric bulk in a region for which the model is relatively trained (Figure 4a) or the information on the lipophilic amide side chain is dominant (Figure 4b).

Therefore, to overcome the steric drawback in the volume approach previously described and complicate the binding site model by explicitly taking into account the electrostatic contribution to the ligand−receptor complementarity as CoMFA does, a different approach has been used in this work. It consists of constructing the surface enclosing a volume common to all the aligned molecules used in its building. The shape obtained is assumed to be complementary to the shape of the receptor site itself. The electrostatic potentials of the ligands are then mapped on such a surface.[29] Since the receptor model is constructed from an aligned bundle of molecules, each surface point is characterized

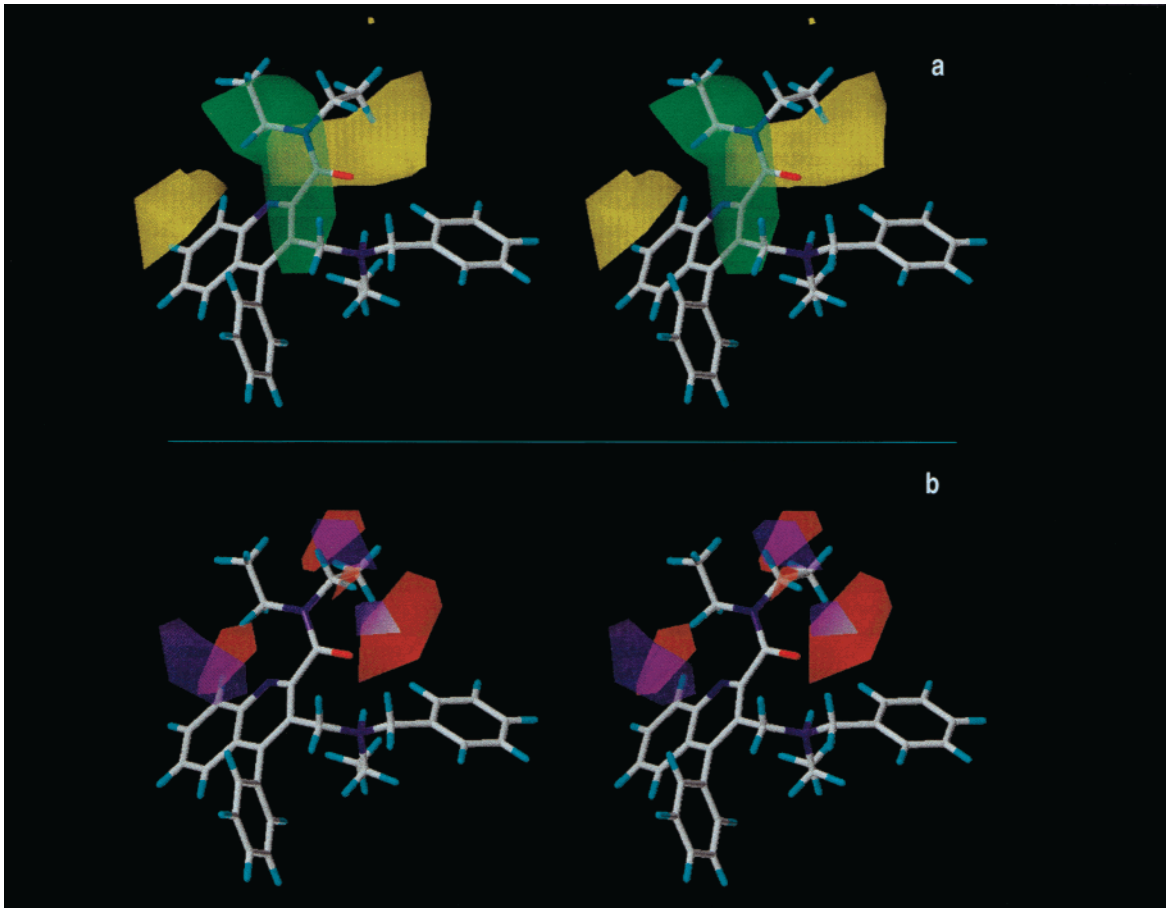

Figure 4. (a) Relaxed stereoview of compound **16** in CoMSIA steric *sdev.*coeff.* contour plot. The yellow contoured areas represent regions in which steric bulk is detrimental for activity; no substucture of this active molecule penetrates this region. Correspondingly, the green contoured area indicates a zone were steric interactions are favored. (b) Relaxed stereoview of compound **16** in CoMSIA electrostatic *sdev.*coeff.* contour plot. The important role of the amide dipole becomes obvious since there is a large red contoured area indicating high electron density in this area favorable to high affinity. On the other hand, the electron-deficient heteroaromatic ring system overlaps partially with the blue region where positive charge is favorable to high affinity.

by a value that is equal but opposite to the average value of the electrostatic potential of the closest atoms in each molecule. Moreover, receptor flexibility can be taken into account by opening the surface model in those parts suggested to be particularly tolerant to substitution by SAFIR analysis. The receptor model obtained is shown in Figure 5a.

The model was built with the same molecules employed in the previous approach—**8f**, **8h**, and **10c**—and the best results were obtained when the alignment was performed by means of dummy atoms (see methods section). The compatibility of each ligand to the model is evaluated, and the energy interaction (E_{inter}) gives a quantitative description of the ligand−receptor site complementarity. The more negative the value of E_{inter}, the more stable the interaction between ligands and receptor.

The QSAR model obtained by considering 34 compounds is

$$pIC_{50} = -1.14(\pm 0.13)E_{inter} + 4.08(\pm 0.37) \quad (3)$$

$$n = 34, \quad r^2 = 0.70, \quad s^2 = 0.38, \quad F = 73.33$$

where ligands **7a**, **7b**, **8c**, **6a**, **13b**, **15b**, **13d**, **13e**, **13f**, and **13g** have been omitted.

All these ligands show low binding affinity to the receptor: **6a**, **13b**, **13d**, **13e**, **13f**, and **13g** have positive interaction energy (repulsive interactions), while **7a**, **7b**, **8c**, and **15b** are overestimated by the model. The statistical indices of this equation are comparable to those of the previous model (eq 2) obtained for all 44 ligands considered. However, this model is able to predict the affinity of compound **16**, as shown in Figure 6 ($pIC_{50\_exp} = 8.39$, $pIC_{50\_calc} = 8.10$).

Finally, the fourth approach used is substantially different from the previous ones. It consists of defining a receptor hypothesis on the basis of pharmacophoric groups shared by a subset of ligands which were chosen as representatives of the set and appropriately located in the 3D space.[30]

In this case, shape is not taken into account, the only consideration concerns whether the ligand possesses the desired characteristics at the defined positions.

The molecules chosen in the building of the hypotheses are **8f**, **8h**, and **11a** (Chart 2). The last one shows high affinity and a peculiarity in the position of the pendant phenyl group. The hypothesis chosen for the evaluation of the ligands studied is shown in Figure 5b and assumes four pharmacophoric groups: (a) one hydrogen bond acceptor (carbonyl group); (b) one aromatic ring corresponding to the pendant phenyl ring; (c) one aromatic ring corresponding to the homocyclic

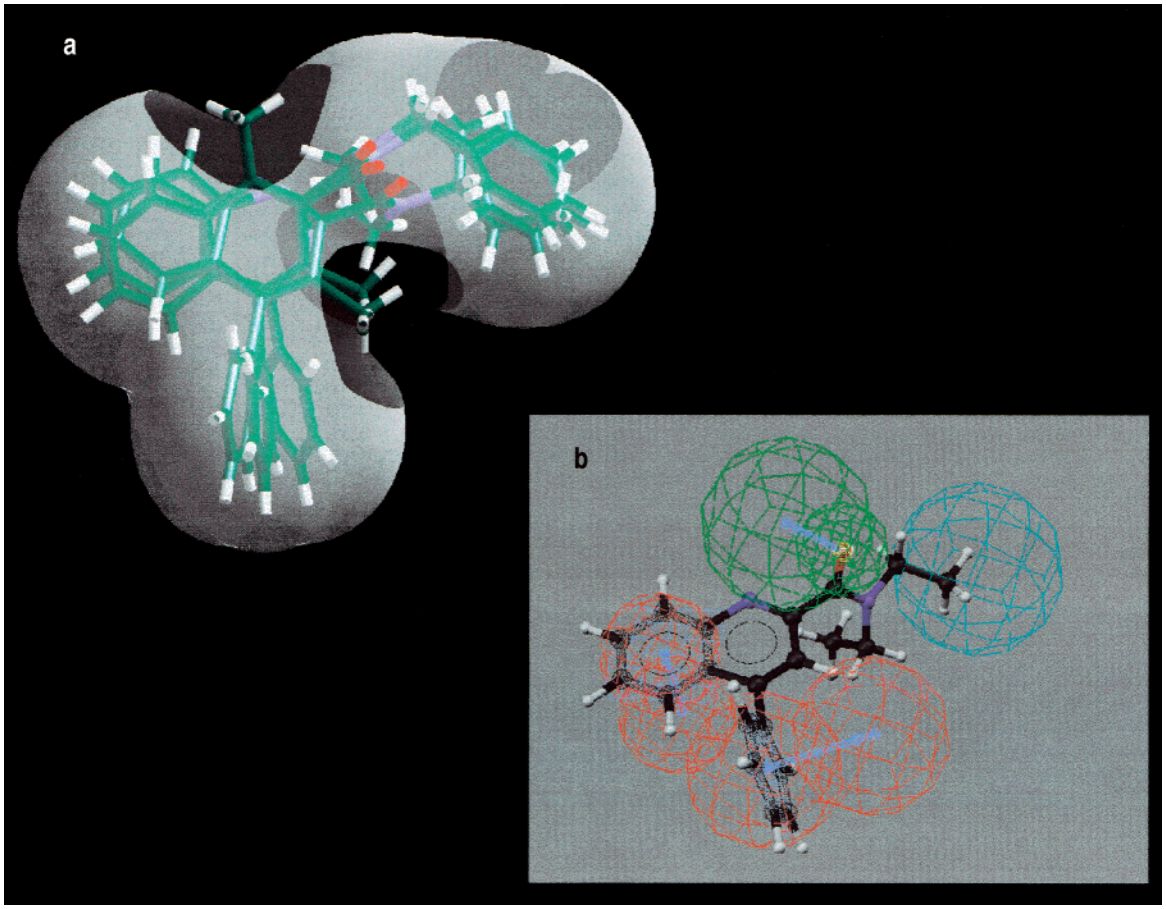

Figure 5. (a) Receptor model of the binding site obtained by overlapping ligands **8f**, **8h**, and **10c**. (b) Pharmacophoric hypothesis obtained by considering ligands **8f**, **8h**, and **11a**. The fitting of compound **4b** to the hypothesis is shown.

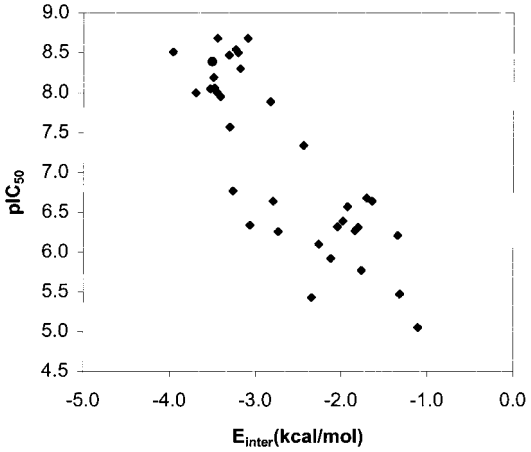

Figure 6. Correlation between the PBR binding affinity (pIC_{50}) and the E_{inter} descriptor. Compound **16** is represented as ●.

ring of the quinoline nucleus; (d) one hydrophobic group for the aliphatic and aromatic chains bound to the amide group.

A score (*Fit*) is then assigned to the molecules under study on the basis of the number of matched functional groups and of the possible penalization for incomplete superimposition or orientation.

On the whole, the descriptor is able to account for 78% of the variance in the receptor affinity for the 44 compounds considered:

$$pIC_{50} = 1.54(\pm 0.13)Fit + 2.36(\pm 0.38) \qquad (4)$$

$$n = 44, \quad r^2 = 0.78, \quad s^2 = 0.28, \quad F = 144.72$$

It can be noted (Figure 7) that ligands showing low and high affinity are clearly clustered in the graph, the threshold for the *Fit* descriptor being equal to 3.

In addition, the activity of compound **16** is adequately predicted ($pIC_{50\_exp} = 8.39$, $pIC_{50\_calc} = 8.12$).

Any attempt to improve the linear QSAR models presented by multiregression analysis of the above-mentioned ad-hoc descriptors with a large variety of electronic and reactivity indexes was unsuccessful. This result seems to support the hypothesis that specific highly directional interactions with a suitable hydrogen-bonding donor amino acid residue of the receptor can easily be achieved from the point of view of the electronic requirements (as the electronic character of the carbonyl group is quite similar in all the ligands considered) once the conformational requirements are satisfied.

(b) Receptor Fitting. (Peripheral Benzodiazepine Receptor Modeling.) The modeling of the 3D structure of the receptor is based on the knowledge of its primary structure (sequence), the results of molecular biophysics and biochemistry studies available in the literature, and the hints from the models obtained with the indirect approaches used.

The alignment of the available PBR sequences, reported in Figure 8, has emphasized the high degree of conservation of some parts of the receptor sequences in

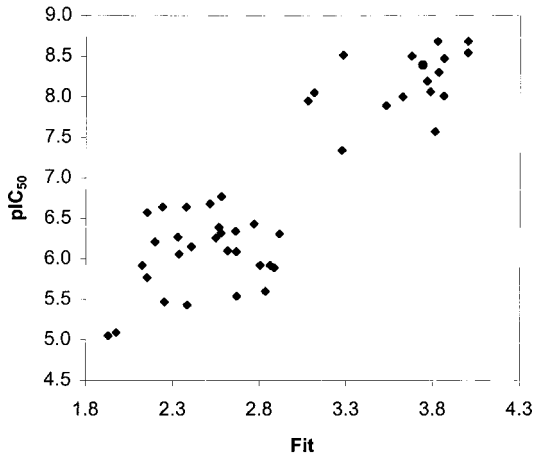

Figure 7. Correlation between the PBR binding affinity (pIC_{50}) and the *Fit* descriptor. Compound **16** is represented as ●.

the different species. The degree of conservation is important in the determination of membrane topology. Highly conserved residues are usually associated with structural or functional roles, while mutated residues (nonconservative mutations) may be important for specificity, or may simply be located in structurally or functionally unimportant portions of the receptor.

Experimental studies for PBR topography determination[5] and the analysis of the hydropathy profile have highlighted the presence of five transmembrane α-helices composed of 21 amino acids, as shown in Figure 8: TM1 (3−23), TM2 (45−65), TM3 (82−102), TM4 (109−129), TM5 (135−155).

The search for analogous proteins with a resolved 3D structure was unsuccessful. In fact, PBR does not show any analogy with other known proteins, apart from a significant relationship with CrtK, a member of the protein family which is responsible for the carotenoid biosynthesis.[31] Unfortunately, the CrtK 3D structure is yet to come. Therefore, the assembly of the five transmembrane helices has thus been carried out with Apolipophorin III (1AEP) as a template. This is a functionally nonrelated lipoprotein of the African migratory locust whose transmembrane topology has been resolved at atomic level.[32]

Only few mutagenesis experiments (chimeric receptors and site-directed mutagenesis) have been published up to now.[5,7,31b,33] They have pointed out that the ligand binding site is located in the loop region that develops outside the mitochondria, in the cell cytoplasm. Thus, we concentrated our efforts in the modeling of this region. In particular, the first cytoplasmic loop that connects the C-terminus of the first helix to the N-terminus of the second is composed of 19 amino acids and seems mostly involved in the interaction with the ligands. The third loop connects the third with the fourth helix and is composed of six residues only. In addition, since deletion studies[33] have shown that the last 13 amino acids of the PBR C-terminus may be deleted without significant effects on the binding of **1** and **2**, only eight terminal amino acids were considered in our 3D model.

To model the first cytoplasmic loop, formed by 19 residues, we searched on a database of protein fragments of known three-dimensional structure. The search was performed on the sequences of the same length of the loop studied whose distances between N-terminus and C-terminus fit the desired range. Among the fragments retrieved, those that showed the residues presumably responsible for the interaction with the ligands located in a favorable mutual position (i.e., near enough to be considered part of the same site) were chosen.

The structural restraints derived by these templates for the first loop and the Apolipophorin III for the transmembrane regions of the receptor were used to obtain several 3D models of PBR. The short third loop and the C-terminal part were modeled ab initio.[20]

Binding Site Spotting. Once a family of 3D PBR models was obtained by randomisation of the Cartesian coordinates,[20] a tentative binding site for the ligands was identified.

Site-directed mutagenesis studies[7] have suggested that residues R24, E29, K39 and L31 may be part of the binding site for **2** (agonist). These residues are located in the first cytoplasmic loop and are conserved through human, bovine, murine, and rat species. The same amino acids play, on the other hand, a marginal role in the interaction with **1**; therefore, this antagonist seems to occupy a similar but not identical binding site. Moreover, studies designed to elucidate the functional and structural properties of TspO of *Rhodobacter sphaeroides*,[31b] which is assumed to be a model for the mammalian PBR, have pointed out the importance of residues L34, K36, W39, and W44 (corresponding to L37, K39, W42, and W47 of the PBR sequence) in the first cytoplasmic loop.

We examined the different models with molecular graphic methods to select the ones which show the maximum complementarity between the position and characteristics of the mutated residues and the pharmacophoric elements of compound **2**. Further selection was made on the basis of energy considerations. We manually docked the agonist into the hypothetical binding site of the different PBR 3D structures, and the complexes we obtained were subjected to minimization. Different orientations of the agonist gave ligand−receptor interaction energies which were taken into account to classify the models and to select the one shown in Figure 9a (binding site of **2**).

Such a model suggests that the binding site is formed by the mutated residues R24, E29, K39, and L31 and by P40, S41, W42, W107, and W161.

The mutation of R32 to glycine lowers the agonist binding constant by a factor of 10. This residue seems to have a structural role in the model. The electrostatic interaction between R32 and the C-terminal part of PBR determines the conformation of the I loop. K39 establishes an electrostatic interaction with the carbonyl oxygen of **2**. It is noteworthy that the Cl-substituted condensed phenyl group is settled in a hydrophobic pocket defined by W42, W107, and W161, while the chlorine atom on the pendant phenyl ring gives rise to dispersive interactions with a more polar environment defined by the ionic couple R24-D157.

On the basis of these results, the receptor hypothesis produced by the pharmacophore approach applied to the ligands studied shows, as far as interactions and the

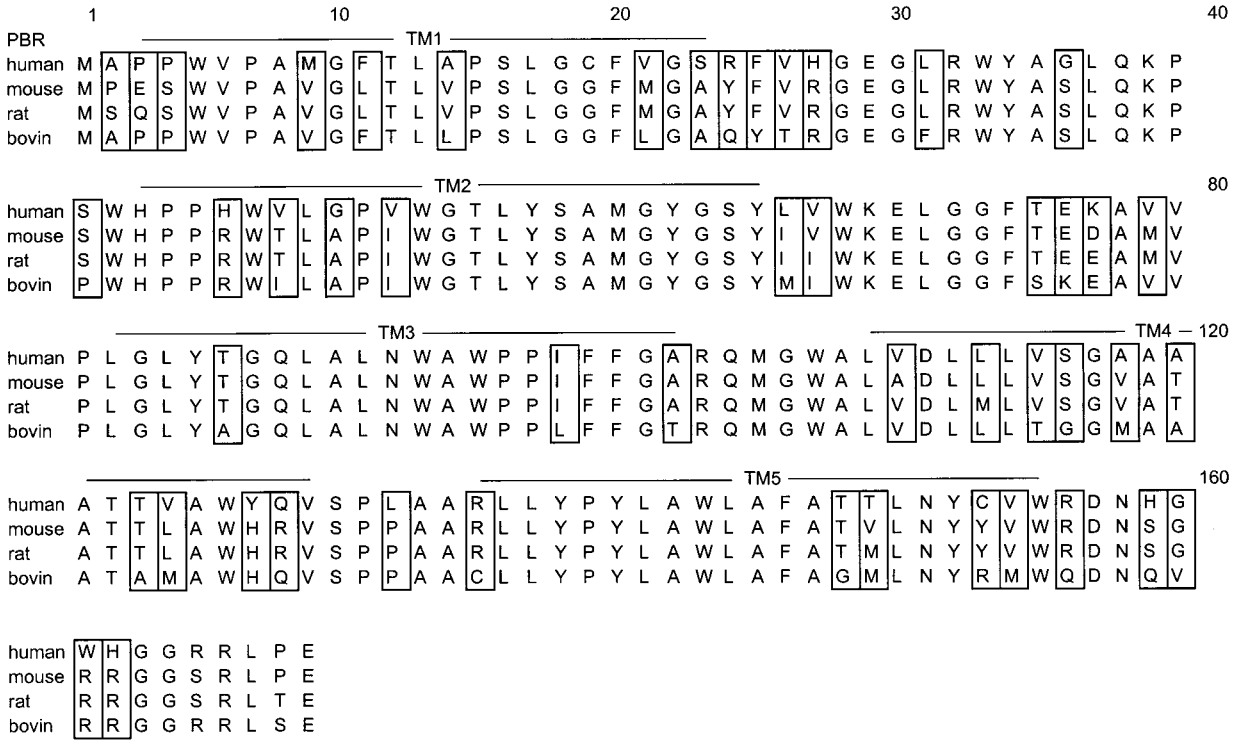

Figure 8. Alignment of the PBR sequences (human, bovine, murine, and rat). The five transmembrane domain have been highlighted. Amino acid residues not conserved among species are boxed.

distances between key elements are concerned, the correspondences listed in Table 5.

The three ligands **8f**, **8h**, and **10c**, used to build the indirect approach supermolecule, were also accommodated in this site and the complexes obtained underwent minimization. Figure 10 shows in detail the interaction modes between two of these ligands (**8f** and **10c**) and the amino acids of the antagonist binding site. The residue S41 has a key role for the directional interaction with the carbonyl moiety, and L31 establishes dispersion interactions with the condensed benzene ring. Mutation of these residues causes a weak decrease of the binding constant of compound **1** (reported in Figure 10 as fitted into its putative binding site). The coherence between the results obtained with the direct approach and the receptor hypothesis built by the indirect approaches, especially concerning the high flexibility regions, can be estimated by comparing Figures 5 and 10d. On the contrary, the indirect approaches seem to allow much more conformational freedom to the position of the carbonyl moiety with respect to the 3D model of the receptor. This might provide a possible explanation for the overestimation of compounds **7a**,**b** and **8c** by eq 3.

Finally, this receptor site is perfectly able to host a PBR ligand structurally unrelated to the previous ones such as alpidem (**3**), the lead compound for the imidazopyridine ligands[34] (Figure 9b).

Moreover, by assuming the same binding modes of **1** for compound **16**, its higher affinity with respect to its analogue **4b** can be explained by the additional interactions of the basic nitrogen in position 3 of the quinoline nucleus with D157 (Figure 9c). Therefore, on the basis of the results obtained by the different approaches, we can suggest site-specific mutations on hPBR which involve amino acids W42, W107, W161, S41, and D157.

Conclusions

Among the different chemical classes of PBR ligands, all the known ligands are highly lipophilic and sometimes their insolubility restricts their use in different pharmacological assays. Because most of our compounds bear a tertiary amino group, which is likely to be protonated at physiological pH, they constitute an original series of water-soluble ligands of PBR sites. In particular, compound **16** represents, to the best of our knowledge, the first example of PBR ligand with affinity in the low nanomolar range bearing a basic nitrogen atom, and it appears to be a new interesting pharmacological tool for the studies of the PBR function and/or an interesting candidate for [^{11}C]-labeling to be used in PET studies.

The combined use of different computational approaches allowed us to obtain a quantitative rationalization of the structural characteristics of peripheral benzodiazepine receptor antagonists and to correlate the interaction effects with the receptor to the functional role of the main structural components. Size and shape descriptors, defined with respect to a supermolecule, turned out to be efficient in describing affinity changes. They quantify the short-range intermolecular interaction contributions to the ligand−receptor interaction, which seem to be, in this case, the determinant ones for the modulation of the affinity. In fact, similar descriptors which also take into account electrostatic interactions have not generated better QSAR models either from the interpretative viewpoint or from the predictive one.

The results obtained suggest that all the ligands considered have the electronic requirements for specific and directional interactions of the carbonyl oxygen with a hydrogen bond donor amino acid of the receptor, but that not all of them can satisfy the conformational

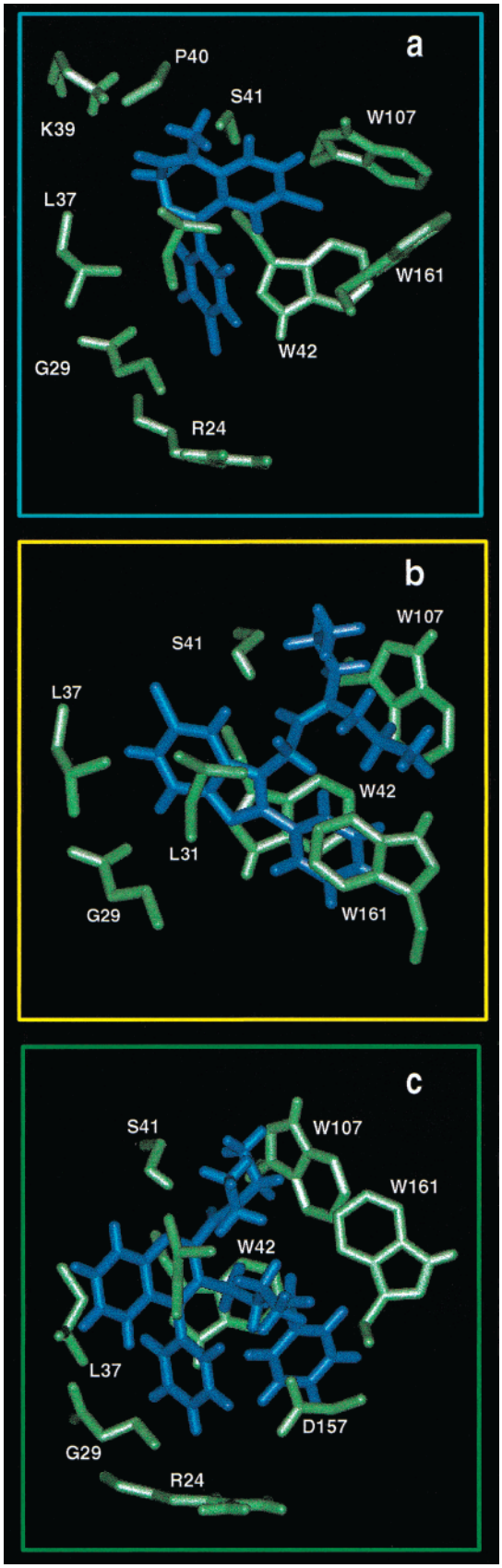

Figure 9. (a) Binding site of agonist **2**. Only residues contributing to the total interaction energy ($E = -42.79$ kca/mol), computed as $E = E_{complex} - E_{ligand}$, with more than 2 kcal/mol are shown. (b) Binding site of compound **3**, structurally unrelated to the previous ligands ($E = -46.72$ kcal/mol). (c) Binding site of compound **16** ($E = -73.93$ kcal/mol).

Table 5. Correspondences between the Results Obtained by Receptor Mapping and Receptor Fitting Approaches

receptor mapping (pharmacophoric hypothesis)	receptor fitting (structural hypothesis)
hydrogen bond acceptor	Ser41
two aromatic rings:	
(1) pendant phenyl	Trp42
(2) condensed ring	Leu31
hydrophobic group	Trp107, Trp161

restraints imposed by the receptor. The receptor hypothesis obtained by the pharmacophore approach has provided, beside a good QSAR model, useful hints for the identification of the antagonist binding site in the three-dimensional structure modeling process of the complexes. The computational simulation of the ligand−receptor interactions gives a detailed picture of the complementarity obtained from the interacting molecules and allows us to speculate on the mechanistic role of the structural components. However, the ligand−receptor models proposed may be challenged when further experimental data are available. All experimental information must be exploited in each step of the modeling procedure, and only an interactive updating process of the developed model/experimental check/experiments project can confirm or invalidate its adequacy or improve its predictivity.

Experimental Section

Melting points were determined in open capillaries on a Gallenkamp apparatus and are uncorrected. Microanalyses were carried out using a Perkin-Elmer 240C elemental analyzer. Merck silica gel 60 (70−230 mesh or 230−400 mesh) was used for column chromatography, and Riedel-de Haen DC-Mikrokarten SI F 37341 were used for TLC. ^{1}H NMR spectra were recorded with a Bruker AC 200 spectrometer in the indicated solvents (TMS as internal standard); the values of the chemical shifts are expressed in ppm and coupling constants (J) in hertz (Hz). Mass spectra (EI, 70 eV) were recorded on a VG 70-250S spectrometer. NMR spectra and elemental analyses were performed by the Dipartimento Farmaco Chimico Tecnologico, Università di Siena. Mass spectra were performed by Centro di Analisi e Determinazioni Strutturali, Università di Siena.

Ethyl 2-[(1,2,3,4-Tetrahydroisoquinoline)-2-methyl]-4-phenylquinoline-3-carboxylate (12b). To a solution of ethyl 2-chloromethyl-4-phenylquinoline-3-carboxylate[13] (0.33 g, 1.0 mmol) in acetonitrile (30 mL) was added sodium iodide, and the resulting mixture was stirred at room temperature for 0.5 h**.** Commercially available 1,2,3,4-tetrahydroisoquinoline (0.16 g, 1.2 mmol) and sodium carbonate (0.42 g, 4.0 mmol) were then added, and the reaction mixture was refluxed for 5 h. After cooling, the mixture was filtered on Celite, and the filtrate was evaporated in vacuo. The residue was dissolved in methylene chloride, and the organic phase was thoroughly washed with H_2O, dried, and evaporated under reduced pressure to give a nearly pure light yellow oil which crystallized on standing. A recrystallization from methanol gave an analytical sample as colorless prisms (yield 70%) melting at 119−121 °C. ^{1}H NMR ($CDCl_3$): 0.59 (t, $J = 7.3$, 3H), 2.8 (bs, 4H), 3.58 (q, $J = 6.9$, 2H), 3.77 (bs, 2H), 4.19 (s, 2H), 6.89−7.10 (m, 4H), 7.25−7.49 (m, 5H), 7.55−7.85 (m, 2H), 8.15 (d, $J = 8.3$, 1H). MS: m/z 422 (M^+, 1). Anal. ($C_{28}H_{26}N_2O_2$) C, H, N.

General Procedures for the Preparation of Hydroxymethyl Carboxamides 20a−e, 21, and 22a−d. Method A. A 2.5 M solution of trimethylaluminum in hexane (0.8 mL, 2.0 mmol) was slowly added to a solution of 2.0 mmol of the suitable amine hydrochloride in 5 mL of dry methylene chloride under nitrogen at room temperature. The mixture was stirred at room temperature for 15 min, and 2.0 mmol of the

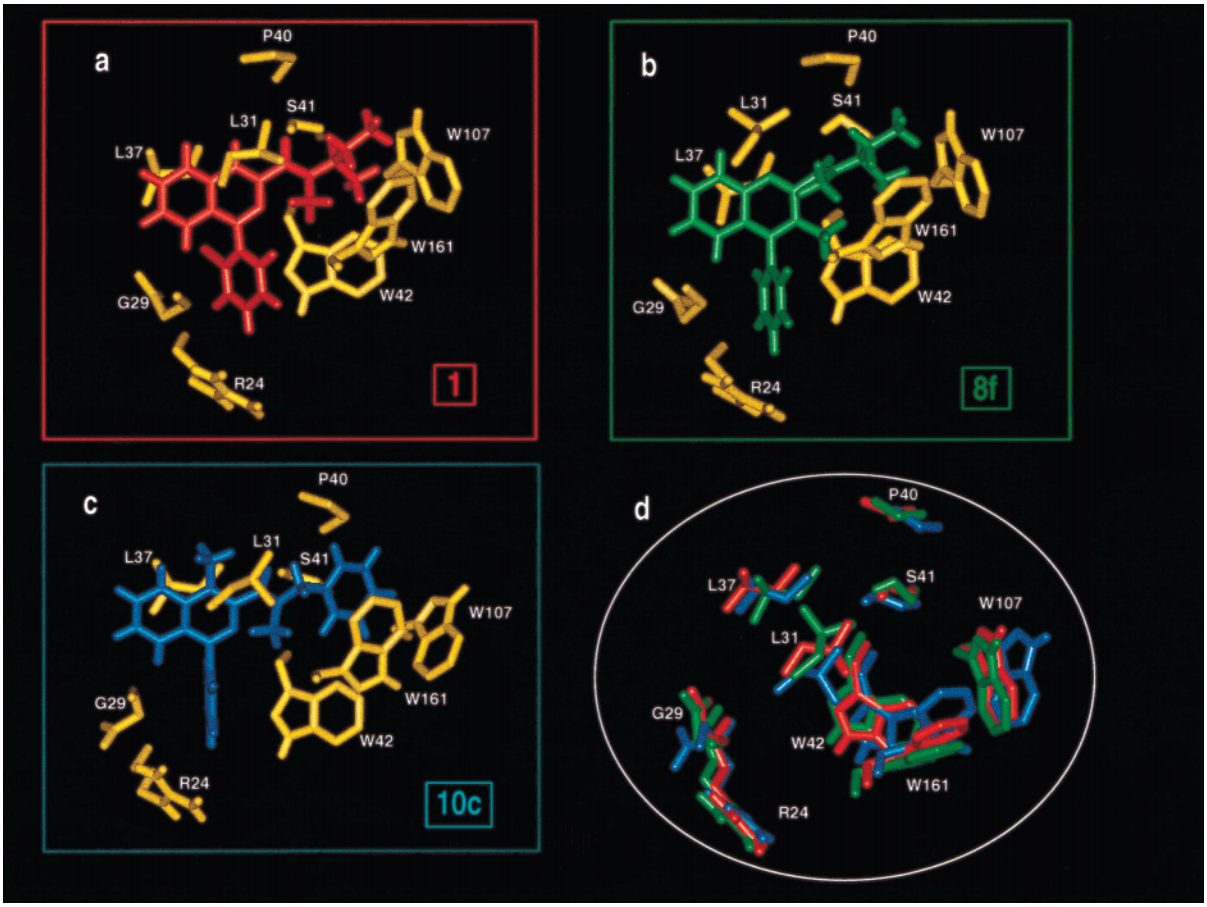

Figure 10. (a) Binding site of **1** ($E = -62.09$ kcal/mol). (b) Binding site of compound **8f** ($E = -66.69$ kcal/mol). (c) Binding site of compound **10c** ($E = -62.16$ kcal/mol). (d) Superimposition of the binding sites of **1**, **8f**, and **10c**, showing the receptor flexibility.

appropriate lactone (**17**−**19**) was added. The mixture was warmed at 25−41 °C under nitrogen until TLC indicated that the reaction was completed. The reaction was carefully quenched with dilute HCl and extracted with methylene chloride. The organic extract was dried ($MgSO_4$) and concentrated to afford the expected hydroxymethyl carboxamide which was purified by flash chromatography with ethyl acetate−methanol (9:1) when necessary. The ^{1}H NMR spectra of those amides, the nitrogen of which bears two different substituents, show the presence of two different rotamers in equilibrium. For the sake of simplification the integral intensities have not been given.

***N,N*-Dimethyl-2-hydroxymethyl-4-phenylquinoline-3-carboxamide (20a).** The title compound was obtained in 80% yield from lactone **17** and dimethylamine hydrochloride. ^{1}H NMR ($CDCl_3$): 2.52 (s, 3H), 2.78 (s, 3H), 4.79 (d, J = 15.6, 1H), 5.05 (m, 2H), 7.33−7.64 (m, 6H), 7.67−7.71 (m, 2H), 8.09 (d, J = 8.1, 1H).

***N,N*-Diethyl-2-hydroxymethyl-4-phenylquinoline-3-carboxamide (20b).** The title compound was obtained in 64% yield from lactone **17** and diethylamine hydrochloride. ^{1}H NMR ($CDCl_3$): 0.72−0.94 (m, 6H), 2.63−2.77 (m, 1H), 2.91−3.13 (m, 2H), 3.57−3.75 (m, 1H), 4.75−5.15 (m, 3H), 7.36−7.58 (m, 6H), 7.67−7.74 (m, 2H), 8.13 (d, J = 8.4, 1H).

***N,N*-Dipropyl-2-hydroxymethyl-4-phenylquinoline-3-carboxamide (20c).** The title compound was obtained in 70% yield from lactone **17** and dipropylamine hydrochloride.^{1}H NMR ($CDCl_3$): 0.59−0.73 (m, 6H), 1.05−1.36 (m, 4H), 2.47−2.59 (m, 1H), 2.80−2.99 (m, 2H), 3.54−3.60 (m, 1H), 4.68−5.07 (m, 3H), 7.34−7.57 (m, 6H), 7.68−7.79 (m, 2H), 8.15 (d, J = 8.5, 1H).

2-Hydroxymethyl-*N*-methyl-*N*-phenyl-4-phenylquinoline-3-carboxamide (20d). The title compound was obtained in 84% yield from lactone **17** and *N*-methylaniline hydrochloride. ^{1}H NMR ($CDCl_3$): 2.90 (s), 3.27 (s), 4.82−5.40 (m), 6.38−6.51 (m), 6.87−6.95 (m), 7.22−7.84 (m), 8.11−8.20 (m).

***N*-(4-Chlorophenyl)-2-hydroxymethyl-*N*-methyl-4-phenylquinoline-3-carboxamide (20e).** The title compound was obtained in 92% yield from lactone **17** and 4-chloro-*N*-methylaniline hydrochloride. ^{1}H NMR ($CDCl_3$): 2.88 (s), 3.20 (s), 4.68−5.20 (m), 6.22−6.26 (m), 6.58 (d, J = 7.5), 6.77−6.95 (m), 7.28−7.80 (m), 8.09−8.22 (m).

***N,N*-Diethyl-3-hydroxymethyl-4-phenylquinoline-2-carboxamide (21).** The title compound was obtained in 98% yield from lactone **18** and diethylamine hydrochloride. ^{1}H NMR ($CDCl_3$): 1.23−1.40 (m, 6H), 3.42 (q, J = 7.1, 2H), 3.69 (q, J = 7.2, 2H), 4.06 (t, J = 5.3, 1H), 4.40 (d, J = 5.4, 2H), 7.35−7.75 (m, 8H), 8.12 (d, J = 8.3, 1H).

***N,N*-Dimethyl-2-hydroxymethylbenzamide (22a).** The title compound was obtained in 55% yield from lactone **19** and dimethylamine hydrochloride. ^{1}H NMR ($CDCl_3$): 2.88 (s, 3H), 3.10 (s, 3H), 4.10 (br s, 1H), 4.49 (s, 2H), 7.15−7.55 (m, 4H).

***N,N*-Diethyl-2-hydroxymethylbenzamide (22b).** The title compound was obtained in 62% yield from lactone **19** and diethylamine hydrochloride. ^{1}H NMR ($CDCl_3$): 1.10 (t, J = 7.1, 3H), 1.28 (t, J = 7.1, 3H), 3.25 (q, J = 7.1, 2H), 3.58 (q, J = 7.1, 2H), 4.52 (s, 2H), 7.23−7.47 (m, 4H).

***N,N*-Dipropyl-2-hydroxymethylbenzamide (22c).** The title compound was obtained in 55% yield from lactone **19** and dipropylamine hydrochloride. ^{1}H NMR ($CDCl_3$): 0.74 (t, J = 7.4, 3H), 1.0 (t, J = 7.4, 3H), 1.50 (q, J = 7.6, 2H), 1.76 (q, J = 7.4, 2H), 3.16 (t, J = 7.5, 2H), 3.50 (t, J = 7.4, 2H), 3.67 (br s, 1H), 4.50 (br s, 2H), 7.20−7.47 (m, 4H).

2-Hydroxymethyl-*N*-methyl-*N*-phenylbenzamide (22d). The title compound was obtained in 89% yield from lactone **19** and *N*-methylaniline hydrochloride. ^{1}H NMR ($CDCl_3$): 2.96 (s), 3.51 (s), 4.66 (s), 5.32 (s), 6.94−7.90 (m).

Method B. The 2-hydroxymethyl carboxamides **20f** and **20g** were prepared by addition of a large excess of the suitable amine (2 mL) to a suspension of lactone **17** (0.26 g, 1.0 mmol) in ethanol (20 mL). The reaction mixture was refluxed for 3−18

h while stirring. After removing the solvent to dryness, the residue was purified by column chromatography by eluting it first with methylene chloride−ethyl acetate (8:2) and then ethyl acetate to obtain pure **20f,g**.

2-Hydroxymethyl-4-phenyl-*N*-propylquinoline-3-carboxamide (20f). The title compound was obtained in 79% yield from lactone **17** and propylamine. ^{1}H NMR ($CDCl_3$): 0.65 (t, J = 7.4, 3H), 1.00−1.25 (m, 2H), 3.06 (q, J = 7.2, 2H), 4.89 (m, 3H), 5.41 (br t, 1H), 7.39−7.79 (m, 8H), 8.10 (d, J = 8.0, 1H).

2-Hydroxymethyl-4-phenyl-*N*-(phenylmethyl)quinoline-3-carboxamide (20g). The title compound was obtained in 84% yield from lactone **17** and benzylamine. ^{1}H NMR ($CDCl_3$): 3.80 (br s, 1H), 4.29 (d, J = 5.5, 2H), 4.96 (s, 2H), 5.68 (br t, 1H), 6.77−6.81 (m, 2H), 7.19−7.26 (m, 3H), 7.37−7.77 (m, 8H), 8.10 (d, J = 8.3, 1H).

General Procedure for the Preparation of Chloromethyl Carboxamides 23a−g, 24, and 25a−d. To a solution of the suitable hydroxymethyl derivative (**20a−g**, **21**, and **22a−d**) (1.25 mmol) in methylene chloride (20 mL) was added thionyl chloride (2 mL, 27.6 mmol), and the resulting mixture was stirred at room temperature for 2−5 h. The solvent was evaporated in vacuo, and the thionyl chloride excess was removed by azeotropic distillation with toluene to give the chloromethyl derivatives in almost quantitative yields as an oily product which was used without any further purification (as judged sufficiently pure by TLC analysis) in the next reaction.

2-Chloromethyl-*N*,*N*-dimethyl-4-phenylquinoline-3-carboxamide (23a). ^{1}H NMR ($CDCl_3$): 2.54 (s, 3H), 2.80 (s, 3H), 4.97 (ABq, J = 11.9, 2H), 7.38−7.55 (m, 6H), 7.69−7.81 (m, 2H), 8.14 (d, J = 8.3, 1H).

2-Chloromethyl-*N*,*N*-diethyl-4-phenylquinoline-3-carboxamide (23b). ^{1}H NMR ($CDCl_3$): 0.76−0.93 (m, 6H), 2.66−2.84 (m, 1H), 3.02−3.20 (m, 2H), 3.52−3.69 (m, 1H), 4.93 (ABq, J = 12.3, 2H), 7.32−7.58 (m, 6H), 7.62−7.87 (m, 2H), 8.16 (d, J = 8.4, 1H).

2-Chloromethyl-*N*,*N*-dipropyl-4-phenylquinoline-3-carboxamide (23c). ^{1}H NMR ($CDCl_3$): 0.65 (t, J = 7.4, 3H), 0.79 (t, J = 7.4, 3H), 1.07−1.46 (m, 4H), 2.54−2.69 (m, 1H), 2.88−3.09 (m, 2H), 3.38−3.52 (m, 1H), 4.90 (ABq, J = 11.2, 2H), 7.35−7.68 (m, 6H), 7.72−7.80 (m, 2H), 8.18 (d, J = 8.3, 1H).

2-Chloromethyl-*N*-methyl-*N*-phenyl-4-phenylquinoline-3-carboxamide (23d). ^{1}H NMR ($CDCl_3$): 2.90 (s), 3.25 (s), 4.81−4.99 (m), 5.30−5.40 (m), 6.38−6.50 (m), 6.86−6.97 (m), 7.20−7.83 (m), 8.10−8.21 (m).

2-Chloromethyl-*N*,*N*-dimethyl-4-phenylquinoline-3-carboxamide (23e). ^{1}H NMR ($CDCl_3$): 2.88 (s), 3.24 (s), 4.80−4.98 (m), 5.28−5.48 (m), 6.39−6.50 (m), 6.78−6.92 (m), 7.27−7.34 (m), 7.39−7.62 (m), 7.69−7.85 (m), 8.11−8.21 (m).

2-Chloromethyl-4-phenyl-*N*-propylquinoline-3-carboxamide (23f). ^{1}H NMR ($CDCl_3$): 0.68 (t, J = 7.4, 3H), 1.08−1.26 (m, 2H), 3.10 (q, J = 7.2, 2H), 5.03 (s, 2H), 5.46 (br t, 1H), 7.39−7.80 (m, 8H), 8.16 (d, J = 8.5, 1H).

2-Chloromethyl-4-phenyl-*N*-(phenylmethyl)quinoline-3-carboxamide (23g). ^{1}H NMR ($CDCl_3$): 4.35 (d, J = 5.6, 2H), 5.05 (s, 2H), 5.64 (br t, 1H), 6.83 (m, 1H), 7.21 (m, 2H), 7.35−7.80 (m, 10H), 8.14 (d, J = 8.4, 1H). MS: m/z 386 (M^+, 68).

3-Chloromethyl-*N*,*N*-diethyl-4-phenylquinoline-2-carboxamide (24). ^{1}H NMR ($CDCl_3$): 1.27−1.38 (m, 6H), 3.28 (q, J = 7.2, 2H), 3.68 (q, J = 7.1, 2H), 4.70 (s, 2H), 7.35−7.76 (m, 8H), 8.13 (d, J = 8.5, 1H). Anal. ($C_{21}H_{21}ClN_2O$) C, H, N.

2-Chloromethyl-*N*,*N*-dimethylbenzamide (25a). ^{1}H NMR ($CDCl_3$): 2.89 (s, 3H), 3.12 (s, 3H), 4.63 (br s, 2H), 7.17−7.58 (m, 4H).

2-Chloromethyl-*N*,*N*-diethylbenzamide (25b). ^{1}H NMR ($CDCl_3$): 1.10 (t, J = 7.1, 3H), 1.28 (t, J = 7.1, 3H), 3.18 (q, J = 7.1, 2H), 3.26−3.57 (br s, 2H), 4.65 (br s, 2H), 7.20−7.48 (m, 4H).

2-Chloromethyl-*N*,*N*-dipropylbenzamide (25c). ^{1}H NMR ($CDCl_3$): 0.76 (t, J = 7.4, 3H), 0.98 (t, J = 7.3, 3H), 1.41−1.82 (m, 4H), 3.05 (t, J = 7.6, 2H), 3.39−3.57 (br s, 2H), 4.64 (br s, 2H), 7.19−7.49 (m, 4H).

2-Chloromethyl-*N*-methyl-*N*-phenyl-benzamide (25d). ^{1}H NMR ($CDCl_3$): 3.01 (s), 3.52 (s), 4.85 (s), 5.33 (s), 6.92−7.95 (m).

General Procedure for the Preparation of Target Carboxamides 13a−g, 15a−d, and 16. To a solution of the appropriate chloromethyl derivative (**23a−g**, **24**, and **25a−d**) (1.5 mmol) in acetonitrile (25 mL) was added sodium iodide (1.5 mmol), and the resulting mixture was stirred at room temperature for 0.5 h**.** *N*-Ethylbenzylamine (0.30 mL, 1.5 mmol) and sodium carbonate (0.64 g, 6.0 mmol) were then added, and the reaction mixture was refluxed for 3 h. After cooling, the mixture was filtered on Celite and the filtrate was evaporated in vacuo. The residue was dissolved in methylene chloride, and the organic phase was thoroughly washed with H_2O until neutral, dried, and evaporated under reduced pressure to give an oily residue which gave the analytical sample after purification by column chromatography with dichloromethane−ethyl acetate (8:2) as the eluent.

***N*,*N*-Dimethyl-2-[(*N*-ethyl)phenylmethylamino]methyl-4-phenylquinoline-3-carboxamide (13a).** The title compound was obtained in 88% yield from **23a**. ^{1}H NMR ($CDCl_3$): 1.02 (t, J = 7.4, 3H), 2.36−2.46 (m, 1H), 2.50 (s, 3H), 2.58−2.68 (m, 1H), 2.71 (s, 3H), 3.60 (d, J = 14.2, 1H), 3.69 (d, J = 12.8, 1H), 3.95 (d, J = 13.9, 1H), 4.41 (d, J = 12.8, 1H), 7.14−7.52 (m, 6H), 7.64−7.74 (m, 2H), 8.15 (d, J = 8.4, 1H). MS: m/z 423 (M^+, 1). Anal. ($C_{28}H_{29}N_3O$) C, H, N.

***N*,*N*-Diethyl-2-[(*N*-ethyl)phenylmethylamino]methyl-4-phenylquinoline-3-carboxamide (13b).** The title compound was obtained in 86% yield from **23b**. ^{1}H NMR ($CDCl_3$): 0.65−0.87 (m, 6H), 1.06 (t, J = 7.4, 3H), 2.51−3.13 (m, 5H), 3.60−4.05 (m, 4H), 4.20 (d, J = 13.7, 1H), 7.10−7.78 (m, 13H), 8.18 (d, J = 8.4, 1H). MS: m/z 451 (M^+, 1.5). Anal. ($C_{30}H_{33}N_3O$) C, H, N.

***N*,*N*-Dipropyl-2-[(*N*-ethyl)phenylmethylamino]methyl-4-phenylquinoline-3-carboxamide (13c).** The title compound was obtained in 74% yield from **23c**. ^{1}H NMR ($CDCl_3$): 0.55−0.78 (m, 6H), 0.88−1.33 (m, 7H), 2.54−2.95 (m, 5H), 3.50−4.21 (m, 5H), 7.19−7.74 (m, 13H), 8.19 (d, J = 8.4, 1H). MS: m/z 479 (M^+, 1.2). Anal. ($C_{32}H_{37}N_3O$) C, H, N.

2-[(*N*-Ethyl)phenylmethylamino]methyl-*N*-methyl-*N*-phenyl-4-phenylquinoline-3-carboxamide (13d). The title compound was obtained in 85% yield from **23d**. ^{1}H NMR ($CDCl_3$): 1.15 (m), 2.56−2.87 (m), 2.91 (s), 3.17 (s), 3.71−3.84 (m), 3.99−4.26 (m), 4.50−4.69 (m), 6.35 (d, J = 7.4), 6.68−6.72 (m), 6.84−6.93 (m), 7.18−7.79 (m), 8.11−8.22 (m). MS: m/z 485 (M^+, 1.3). Anal. ($C_{33}H_{31}N_3O$) C, H, N.

2-[(*N*-Ethyl)phenylmethylamino]methyl-*N*-methyl-*N*-(4-chlorophenyl)-4-phenylquinoline-3-carboxamide (13e). The title compound was obtained in 69% yield from **23e**. ^{1}H NMR ($CDCl_3$): 1.15 (m), 2.53−2.90 (m), 2.92 (s), 3.11 (s), 3.67−3.82 (m), 3.96−4.24 (m), 4.40−4.60 (m), 6.38 (d, J = 7.4), 6.62−6.94 (m), 7.26−7.94 (m), 8.11−8.22 (m). MS: m/z 519 (M^+, 1). Anal. ($C_{33}H_{30}ClN_3O$) C, H, N.

2-[(*N*-Ethyl)phenylmethylamino]methyl-*N*-propyl-4-phenylquinoline-3-carboxamide (13f). The title compound was obtained in 51% yield from **23f**. ^{1}H NMR ($CDCl_3$): 0.7 (t, J = 7.4, 3H), 1.03−1.24 (m, 5H), 2.67 (q, J = 6.9, 2H), 3.05−3.15 (m, 2H), 3.71 (s, 2H), 4.15 (s, 2H), 6.39 (br t, 1H), 7.10−7.76 (m, 13H), 8.14 (d, J = 8.4, 1H). MS: m/z 437 (M^+, 2.5). Anal. ($C_{29}H_{31}N_3O$) C, H, N.

2-[(*N*-Ethyl)phenylmethylamino]methyl-*N*-phenylmethyl-4-phenylquinoline-3-carboxamide (13g). The title compound was obtained in 34% yield from **23g**. ^{1}H NMR ($CDCl_3$): 1.09 (t, J = 7.2, 3H), 2.64 (q, J = 7.0, 2H), 3.69 (s, 2H), 4.15 (s, 2H), 4.31 (d, J = 4.6, 2H), 6.87 (br t, 1H), 6.89−6.91 (m, 1H), 7.04 (s, 5H), 7.20−7.38 (m, 6H), 7.42−7.55 (m, 5H), 7.66−7.33 (m, 1H), 8.12 (d, J = 8.5, 1H). MS: m/z 485 (M^+, 4). Anal. ($C_{33}H_{31}N_3O$) C, H, N.

***N*,*N*-Dimethyl-2-[(*N*-ethyl)phenylmethylamino]methylbenzamide (15a).** The title compound was obtained in 52% yield from **25a**. ^{1}H NMR ($CDCl_3$) 1.02 (t, J = 6.9, 3H), 2.45 (q, J = 7.0, 2H), 2.78 (s, 3H), 3.11 (s, 3H), 3.56 (s, 4H), 7.11−7.36 (m, 8H), 7.60 (d, J = 7.7, 1H); MS m/z 296 (M^+, 1). Anal. ($C_{19}H_{24}N_2O$). C, H, N.

***N,N*-Diethyl-2-[(*N*-ethyl)phenylmethylamino]methylbenzamide (15b).** The title compound was obtained in 48% yield from **25b**. ^{1}H NMR ($CDCl_3$): 0.90−1.11 (m, 6H), 1.25 (t, J = 7.1, 3H), 2.47 (q, J = 7.0, 2H), 3.07 (q, J = 7.0, 2H), 3.24−3.90 (br s, 6H), 7.11−7.36 (m, 8H), 7.68 (d, J = 7.7, 1H). MS: m/z 324 (M^+, 1). Anal. ($C_{21}H_{28}N_2O$) C, H, N.

***N,N*-Dipropyl-2-[(*N*-ethyl)phenylmethylamino]methylbenzamide (15c).** The title compound was obtained in 40% yield from **25c**. ^{1}H NMR ($CDCl_3$): 0.66 (t, J = 7.1, 3H), 0.94−1.07 (m, 6H), 1.39−1.61 (m, 2H), 1.68−1.82 (m, 2H), 2.48 (q, J = 7.0, 2H), 2.96 (t, J = 7.4, 2H), 3.36−3.56 (m, 6H), 7.10−7.36 (m, 8H), 7.72 (d, J = 7.7, 1H). MS: m/z 352 (M^+, 2). Anal. ($C_{23}H_{32}N_2O$) C, H, N.

2-[(*N*-Ethyl)phenylmethylamino]methyl-*N*-methyl-*N*-phenylbenzamide (15d). The title compound was obtained in 58% yield from **25d**. ^{1}H NMR ($CDCl_3$): 1.06 (t, J = 7.0, 3H), 2.48 (q, J = 6.9, 2H), 3.46−3.75 (m, 7H), 7.07−7.58 (m, 14H). Anal. ($C_{24}H_{26}N_2O$) C, H, N.

***N,N*-Diethyl-3-[(*N*-ethyl)phenylmethylamino]methyl-4-phenylquinoline-2-carboxamide (16).** The title compound was obtained in 78% yield from **24**. ^{1}H NMR ($CDCl_3$): 0.75 (t, J = 7.3, 3H), 1.31−1.40 (m, 6H), 2.25 (q, J = 6.2, 2H), 3.27 (q, J = 6.9, 2H), 3.41 (s, 2H), 3.68 (q, J = 6.9, 2H), 3.80 (s, 2H), 7.05−7.50 (m, 12H), 7.60−7.68 (m, 1H), 8.09 (d, J = 8.3, 1H). MS (FAB): m/z 452 (M + 1, 100). Anal. ($C_{30}H_{33}N_3O\cdot 0.25H_2O$) C, H, N.

2-Bromomethyl-4-phenylquinoline (28). A mixture of 2-methyl-4-phenylquinoline[16a] (1.0 g, 4.57 mmol) in carbon tetrachloride (40 mL) with *N*-bromosuccinimide (0.81 g, 4.57 mmol) and dibenzoyl peroxide (0.2 g, 0.8 mmol) was refluxed for 72 h. The solvent was then evaporated in vacuo, and the residue was diluted with small portions of the same solvent and filtered. The filtrate was concentrated under reduced pressure, and the residue was purified by column chromatography eluting with *n*-hexane−ethyl acetate (9:1) to give compound **28** (yield 51%) which was used as such in the next step. ^{1}H NMR ($CDCl_3$) 4.72 (s, 2H), 7.42−7.62 (m, 7H), 7.65−7.80 (m, 1H), 7.90 (d, J = 8.1, 1H), 8.12 (d, J = 8.1, 1H).

2-[(*N*-Ethyl)phenylmethylamino]methyl-4-phenylquinoline (13h). A mixture of 2-bromomethyl derivative **28** (0.3 g, 1.0 mmol) and *N*-ethylbenzylamine (0.89 mL, 6.0 mmol) in ethanol (20 mL) was heated at reflux until the starting material disappeared (2.5 h). The solvent was removed in vacuo and the residue dissolved in diethyl ether. The organic phase was washed to neutrality, dried, and evaporated to dryness. Purification of the residue by flash chromatography with *n*-hexane−ethyl acetate (8:2) as the eluent gave an analytical sample of **13h** as a light yellow oil (0.34 g, yield 96%). ^{1}H NMR ($CDCl_3$): 1.10 (t, J = 7.0, 3H), 2.62 (q, J = 7.0, 2H), 3.69 (s, 2H), 3.95 (s, 2H), 7.19−7.51 (m, 11H), 7.64−7.71 (m, 2H), 7.86 (d, J = 8.0, 1H), 8.10 (d, J = 8.3, 1H). Anal. ($C_{25}H_{24}N_2$) C, H, N.

Preparation of 2-Methyl-4-phenylquinoline-3-carboxylic Acid (27). A mixture of ester **26**[15] (5.9 g, 2.0 mmol), potassium hydroxyde (3.0 g, 53 mmol), ethanol (40 mL), and water (4 mL) was refluxed for 24 h. After cooling and acidification with glacial acetic acid, the reaction mixture was concentrated under reduced pressure and the product was precipitated by addition of water. It was collected, washed with water until neutral, dried, and recrystallized from a mixture of methanol/2-propanol to yield acid **27** (3.5 g, yield 73%) as colorless crystals melting at 268 °C (lit.[16] 265−267 °C). ^{1}H NMR (DMSO-d_6): 2.67 (s, 3H), 7.32−7.51 (m, 7H), 7.61−7.68 (m, 1H), 8.00 (d, J = 8.4, 1H), 13.29 (br s, 1H).

General Procedure for the Preparation of 2-Methyl-4-Phenylquinoline-3-Carboxamides (14a−c). Phosphorus pentachloride (0.45 mL, 3,4 mmol) was added to a suspension of the acid **27** (0.91 g, 3.4 mmol) in methylene chloride (20 mL) cooled to −20 °C. After being stirred for 30 min at this temperature, this mixture was added to a stirred solution of the suitable amine (10 mmol) in methylene chloride (25 mL) layered with 10% aqueous sodium carbonate (10 mL) and ice (5 g). The two-phase mixture was stirred for 30 min and followed by the addition of sodium carbonate solution (10 mL) for another 15 min. The methylene chloride layer was separated, dried, and filtered. Another portion of amine (10 mmol) was added to the solution, and this mixture was heated to reflux for 20 min, diluted with methylene chloride, and washed with water. The organic phase was dried and evaporated to afford a residue which after purification by column chromatography with methylene chloride−ethyl acetate (1:1) gave an oily product which crystallized on standing.

***N,N*-Diethyl-2-methyl-4-phenylquinoline-3-carboxamide (14a).** Yield 85%; mp 97−99 °C. ^{1}H NMR ($CDCl_3$): 0.73 (t, J = 7.1, 3H), 0.87 (t, J = 7.2, 3H), 2.63−2.81 (m, 4H), 2.89−3.17 (m, 2H), 3.61−3.79 (m, 1H), 7.30−7.74 (m, 8H), 8.13 (d, J = 8.2, 1H). MS: m/z 318 (M^+, 22). Anal. ($C_{21}H_{22}N_2O$) C, H, N.

***N,N*-Dipropyl-2-methyl-4-phenylquinoline-3-carboxamide (14b).** Yield 84%, mp 110−111 °C. ^{1}H NMR ($CDCl_3$): 0.66 (m, 6H), 1.08−1.37 (m, 4H), 2.50−2.64 (m, 1H), 2.73−3.02 (m, 5H), 3.51−3.65 (m, 1H), 7.29−7.73 (m, 8H), 8.06 (d, J = 8.3, 1H). MS: m/z 346 (M^+, 20). Anal. ($C_{23}H_{26}N_2O$) C, H, N.

***N*-Methyl-*N*-phenyl-2-methyl-4-phenylquinoline-3-carboxamide (14c).** Yield 83%; mp 129−131 °C. ^{1}H NMR ($CDCl_3$): 2.88 (s), 2.95 (s), 3.23 (s), 6.38 (m), 6.52 (m), 6.85 (m), 6.96 (m), 7.23−7.75 (m), 7.98−8.18 (m). MS m/z 352 (M^+, 32). Anal. ($C_{24}H_{20}N_2O$) C, H, N.

In Vitro Binding Assays. Male CRL:CD(SD)BR (Charles River Italia, Calco, CO, Italy) rats were killed by decapitation, and their brains were rapidly dissected into the various areas and stored at −80 °C until the day of assay. The binding assays were performed as described by Cantoni et al.[35] The frozen cortices were homogenized in 50 vols of ice-cold phosphate-buffered saline (PBS) (50 mM, pH 7.4) containing 100 mM NaCl, using an Ultra Turrax TP-1810 (2 × 20 s). The homogenate was centrifuged for 10 min at 1000*g* at 4 °C (Beckman model J-21B refrigerated centrifuge). The pellet was washed three more times by resuspension in the same volume of fresh buffer and centrifuged again at 50000*g* for 10 min. The pellet obtained was finally resuspended in the incubation buffer (PBS) just before the binding assay.

[^{3}H]PK11195 (s.a. 86.4 Ci/mmol, NEN) binding was assayed in a final incubation volume of 1.0 mL, consisting of 0.5 mL of membrane suspension, 0.5 mL of [^{3}H]-ligand, and 20 μL of displacing agent or solvent. Tissue concentration and [^{3}H]-PK11195 final concentration were 2.3 mg tissue/sample and 1 nM, respectively.

Incubations (120 min at 4 °C) were stopped by rapid filtration under vacuum through GF/B fiber filters which were then washed with 12 mL (3 × 4 mL) of ice-cold PBS by means of a Brandel M-48RP cell harvester.

Nonspecific binding was assayed in the presence of PK11195 (1 μM).

Dried filters were immersed in vials containing 4 mL of Filter Count (Packard) liquid scintillation cocktail for the measurement of trapped radioactivity with a Packard LKB 1214 RACKBETA liquid scintillation spectrometer at a counting efficiency of about 60%. The concentration of the test compounds that inhibited [^{3}H]ligand binding by 50% (IC_{50}) was determined by means of the Allfit [36] program with six concentrations of the displacers, each performed in triplicate.

Acknowledgment. The authors are grateful to Prof. Stefania D'Agata D'Ottavi for the careful reading of the manuscript. Dr Gianluca Giorgi (C.I.A.D.S., Siena) is also acknowledged for the recording of mass spectra. A.M. is grateful to Prof. C. G. Wermuth for the scientifically fruitful months spent at CNRS (LPM) in Strasbourg. M.C.M. and M.S. are especially grateful to CICAIA (Centro Interdipartimentale Calcolo Automatico e Informatica Applicata) for the Cerius^2 program. This work was financially supported by Italian MURST (ex 60% and ex 40% funds) and was partially funded by a contract with NFCR.

References

(1) (a) Verma, A.; Snyder, S. H. Peripheral Type Benzodiazepine Receptors. *Annu. Rev. Pharmacol. Toxicol.* **1989**, *29*, 307−322. (b) Saano, V.; Rägo, L.; Räty, M. Peripheral Benzodiazepine Binding Sites. *Pharmacol. Ther.* **1989**, *41*, 503−514. (c) Gavish, M.; Katz, Y.; Bar-Ami, S.; Weizman, R. Biochemical, Physiological, and Pathological Aspects of the Peripheral Benzodiazepine Receptor. *J. Neurochem.* **1992**, *58*, 1589−1601.

(2) *Peripheral Benzodiazepine Receptors*; Giesen-Crouse, E., Ed.; Academic Press: London, 1993.

(3) Kozikowski, A. P.; Ma, D.; Brewer, J.; Sun, S.; Costa, E.; Romeo, E.; Guidotti A. Chemistry, Binding Affinities, and Behavioral Properties of a New Class of "Antineophobic" Mitochondrial DBI Receptor Complex (mDRC) Ligands. *J. Med. Chem.* **1993**, *36*, 2908−2920 and references therein.

(4) Sprengel, R.; Werner, P.; Seeburg, P. H.; Mukhin, A. G.; Santi, M. R.; Grayson, D. R.; Guidotti, A.; Krueger, K. E. Molecular Cloning and Expression of cDNA Encoding a Peripheral-Type Benzodiazepine Receptor. *J. Biol. Chem.* **1989**, *264*, 20415−20421.

(5) Joseph-Liauzun, E.; Delmas, P.; Shire, D.; Ferrara, P. Topological Analysis of the Peripheral Benzodiazepine Receptor in Yeast Mitochondrial Membrane Supports a Five-Transmembrane Structure. *J. Biol. Chem.* **1998**, *273*, 2146−2152.

(6) Bernassau, J. M.; Reversat, J. L.; Ferrara, P.; Caput, D.; Le Fur, G. A 3D Model of the Peripheral Benzodiazepine Receptor and its Implication in Intramitochondrial Cholesterol Transport. *J. Mol. Graphics* **1993**, *11*, 236−244.

(7) Farges, R.; Joseph-Liauzun, E.; Shire, D.; Caput, D.; Le Fur, G.; Ferrara, P. Site-Directed Mutagenesis of the Peripheral Benzodiazepine Receptor: Identification of Amino Acids Implicated in the Binding Site of Ro5-4864. *Mol. Pharmacol.* **1994**, *46*, 1160−1167.

(8) Bourguignon, J. J. Endogenous and Synthetic Ligands of Mitochondrial Benzodiazepine Receptors: Structure-Affinity Relationships. In *Peripheral Benzodiazepine Receptors*; Giesen-Crouse, E., Ed.; Academic Press: London, 1993; pp 59−85.

(9) Georges, G.; Vercauteren, D. P.; Vanderveken, D. J.; Horion, R.; Evrard, G.; Fripiat, J. G.; Andre, J. M.; Durant, F. Structural and Electronic Analysis of Peripheral Benzodiazepine Ligands: Description of the Pharmacophoric Elements for Their Receptor. *Int. J. Quantum Chem., Quantum Biol. Symp.* **1990**, 17, 1−25.

(10) Anzini, M.; Cappelli, A.; Vomero, S.; Cagnotto, A.; Skorupska, M. Synthesis and Benzodiazepine Receptor Affinity of 2,3-Dihydro-9-phenyl-1*H*-pyrrolo[3,4-*b*]quinolin-1-one and 3-Carbethoxy-4-phenylquinoline Derivatives. *Farmaco* **1992**, *47*, 191−202.

(11) Cappelli, A.; Anzini, M.; Vomero, S.; De Benedetti, P. G.; Menziani, M. C.; Giorgi, G.; Manzoni, C. Mapping the Peripheral Benzodiazepine Receptor Binding Site by Conformationally Restrained Derivatives of 1-(2-Chlorophenyl)-*N*-methyl-*N*-(1-methylpropyl)-3-isoquinolinecarboxamide (PK11195). *J. Med. Chem.* **1997**, *40*, 2910−2921.

(12) Matarrese, M.; Soloviev, D.; Cappelli, A.; Todde, S.; Moresco, R. M.; Anzini, M.; Vomero, S.; Sudati, F.; Carpinelli, A.; Perugini, F.; Galli Kienle, M.; Fazio, F. Synthesis of the Novel [^{11}C]-Labelled Quinoline Carboxamides: Analogues of PK-11195 as Putative Radioligands for PET Studies of Peripheral Type Benzodiazepine Receptors. *J. Labelled Compd. Radiopharm.* **1999**, *42*, S397−S399.

(13) Anzini, M.; Cappelli, A.; Vomero, S. Synthesis of 2-Substituted-2,3-dihydro-9-phenyl-1*H*-pyrrolo[3,4-*b*]quinolin-3-ones as Potential Peripheral Benzodiazepine-receptor Ligands. *Heterocycles* **1994**, *38*, 103−111 and references therein.

(14) (a) Basha, A.; Lipton, M.; Weinreb, S. M. A Mild, General Method for Conversion of Ester to Amides. *Tetrahedron Lett.* **1977**, *48*, 4171−4174. (b) Levin, J. I.; Turos, E.; Weinreb, S. M. An Alternative Procedure for the Aluminum-Mediated Conversion of Esters to Amides. *Synth. Commun.* **1982**, *12*, 989−993.

(15) Fehnel, E. A. Friedlander Syntheses with *o*-Aminoaryl Ketones. III. Acid-Catalyzed Condensations of *o*-Aminobenzophenone with Polyfunctional Carbonyl Compounds (1,2). *J. Heterocycl. Chem.* **1967**, *4*, 565−570.

(16) (a) Fehnel, E. A. Friedlander Syntheses with *o*-Aminoaryl Ketones. I. Acid-Catalyzed Condensations of *o*-Aminobenzophenone with Ketones. *J. Org. Chem.* **1966**, *31*, 2899−2902. (b) Fehnel, E. A.; Cohn, D. E. Friedlander Syntheses with *o*-Aminoaryl Ketones. II. Structure of the Product Formed in the Condensation of *o*-Aminobenzophenone with Acetylacetone. *J. Org. Chem.* **1966**, *31*, 3852−3854.

(17) Dewar, M. J. S.; Zoebisch, E. G.; Healey, E. F.; Stewart, J. J. P. AM1: A New General Purpose Quantum Mechanical Molecular Model. *J. Am. Chem. Soc.* **1985**, *107*, 3902−3909.

(18) Molecular Simulations Inc., 16 New England Executive Park, Burlington, MA, 01803-5297.

(19) Wyvill, G.; McPheeters, C.; Wyvill, B. Data Structures for Soft Objects. *Visual Comput.* **1986**, *2*, 227−234.

(20) Sali, A., Blundell, T. L. Comparative Protein Modeling by Satisfaction of Spatial Restraints. *J. Mol. Biol.* **1993**, *234*, 779−815.

(21) Brooks, B. R.; Bruccoleri, R. E.; Olafson, B. D.; States, D. J.; Swaminathan, S.; Karplus, M. CHARMM: A Program for Macromolecular Energy, Minimization and Dynamics Calculations. *J. Comput. Chem.* **1983**, *4*, 187−217.

(22) Bowie, J. U.; Luthy, R.; Eisenberg, D. A Method to Identify Protein Sequences that Fold into a Known Three-dimensional Structure. *Science* **1991**, *253*, 164−170.

(23) Cramer R. D.; Pattersn, D. E.; Bunce, J. D. Comparative Molecular Field Analysis (CoMFA). 1. Effect of Shape on Binding of Steroids to Carrier Proteins. *J. Am. Chem. Soc.* **1988**, *110*, 5959−5967.

(24) Hagen, B. 3D-QSAR Studies of Ligands of Peripheral Benzodiazepine Receptors. Diploma Thesis, University of Innsbruck, 1999.

(25) Tripos Associates Inc., St. Louis, MO.

(26) Wold, S.; Ruhe, A.; Wold, H.; Dunn, W. J. The Covariance Problem in Linear Regression. The Partial Least Squares (PLS) Approach to Generalized Inverses. *SIAM J. Sci. Stat. Comp.* **1984**, *5*, 735−743.

(27) Klebe, G. Comparative Molecular Similarity Indices: CoMSI. In *3D QSAR in Drug Design*; Kubinyi, H., Folkers, G., Martin, Y., Eds.; Kluver Academic Publisher: Great Britain, 1998, Vol. 3, pp 87−104.

(28) (a) Menziani, M. C.; De Benedetti, P. G.; Karelson, M. Theoretical Descriptors in Quantitative Structure-Affinity and Selectivity Relationship Study of Potent N4-substituted Arylpiperazine 5-HT$_{1A}$ Receptor Antagonists. *Bioorg. Med. Chem.* **1998**, *6*, 535−550. (b) Menziani, M. C.; Montorsi, M.; De Benedetti, P. G.; Karelson, M. Relevance of Theoretical Molecular Descriptors in Quantitative Structure−Activity Relationship Analysis of α_1-Adrenergic Receptor Antagonists. *Bioorg. Med. Chem.* **1999**, *7*, 2437−2451.

(29) Hahn, M. Receptor Surface Models. 1. Definition and Construction. *J. Med. Chem.* **1995**, *38*, 2080−2090.

(30) Pan, C. P.; Hirashima, A.; Kuwano, E.; Eto, M. Three-dimensional Pharmacophore Hypoteses for the Locust Neuronal Octopamine Receptor (OAR). 1. Antagonists. *J. Mol. Model.* **1997**, *3*, 455−463.

(31) (a) Yeliseev, A.; Krueger, K. E.; Kaplan, S. A Mammalian Mitochondrial Drug Receptor Functions as a Bacterial "Oxygen" Sensor. *Proc. Natl. Acad. Sci. U.S.A.* **1997**, *94*, 5101−5106. (b) Yeliseev, A. A.; Kaplan, S. TspO of *Rhodobacter sphaeroides*. *J. Biol. Chem.* **2000,** *275*, 5657−5667.

(32) Breiter, D. R.; Kanost, M. R.; Benning, M. M.; Wesenberg, G.; Law, J. H.; Wells, M. A.; Rayment, I.; Holden, H. M. Molecular Structure of an Apolipoprotein Determined at 2.5 Å Resolution. *Biochemistry* **1991**, *30*, 603−608.

(33) Farges, R.; Joseph-Liauzun, E.; Shire, D.; Caput, D.; Le Fur, G.; Loison, G.; Ferrara, P. Molecular basis for the Different Binding Properties of Benzodiazepines to Human and Bovine Peripheral-type Benzodiazepine Receptors. *FEBS Lett.* **1993**, *335*, 305−308.

(34) (a) Trapani, G.; Franco, M.; Ricciardi, L.; Latrofa, A.; Genchi, G.; Sanna, E.; Tuveri, F.; Cagetti, E.; Biggio, G.; Liso, G. Synthesis and Binding Affinity of 2-Phenylimidazo[1,2-*a*]pyridine Derivatives for both Central and Peripheral Benzodiazepine Receptors. A New Series of High-Affinity and Selective Ligands for the Peripheral Type. *J. Med. Chem.* **1997**, *40*, 3109−3118. (b) Trapani, G.; Franco, M.; Latrofa, A.; Ricciardi, L.; Carotti, A.; Serra, M.; Sanna, E.; Biggio, G.; Liso, G. Novel 2-Phenylimidazo[1,2-*a*]pyridine Derivatives as Potent and Selective Ligands for Peripheral Benzodiazepine Receptors: Synthesis, Binding Affinity, and in Vivo Studies. *J. Med. Chem.* **1999**, *42*, 3934−3941.

(35) Cantoni, L.; Rizzardini, M.; Skorupska, M.; Cagnotto, A.; Categoni, A.; Pecora, N.; Frigo, L.; Ferrarese, C.; Mennini, T. Hepatic Protoporphyria is Associated with a Decrease in Ligand Binding for Mitochondrial Benzodiazepine Receptors in the Liver. *Biochem. Pharmacol.* **1992**, *44*, 1159−1164.

(36) Munson, P. G.; Roadbard, D. *Computers in Endocrinology*; Raven Press: New York, 1984; pp 117−145.

JM0009742